Theses and Dissertations   Theses, Dissertations, and Senior Projects

1-1-2018

Comparing Source Rock Maturity With Pore Size Distribution And Fluid Saturation In The Bakken-Three Forks Petroleum System, Williston Basin, North Dakota

Adedoyin Suleman Adeyilola

[How does access to this work benefit you? Let us know!](#)

Follow this and additional works at: https://commons.und.edu/theses

Part of the Geology Commons

COMPARING SOURCE ROCK MATURITY WITH PORE SIZE DISTRIBUTION AND
FLUID SATURATION IN THE BAKKEN-THREE FORKS PETROLEUM SYSTEM,
WILLISTON BASIN, NORTH DAKOTA

by

Adedoyin Suleman Adeyilola
Bachelor of Science, Obafemi Awolowo University, 2012

A Thesis

Submitted to the Graduate Faculty

of the

University of North Dakota

in partial fulfillment of the requirements

for the degree of
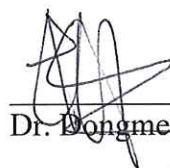
Master of Science

Grand Forks, North Dakota

December
2018

This thesis, submitted by Adedoyin S. Adeyilola in partial fulfillment of the requirements for the Degree of Master of Science from the University of North Dakota, has been read by the faculty Advisory committee under whom the work has been done and is hereby approved.
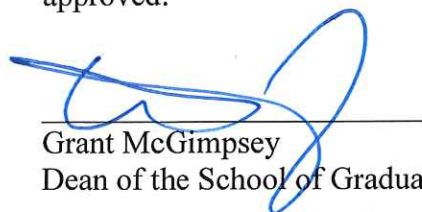
Dr. Stephan H. Nordeng, Chairperson

Dr. Dongmei Wang

11/16/18

Dr. Mehdi Ostadhassan

This thesis is being submitted by the appointed advisory committee as having met all of the requirements of the School of Graduate Studies at the University of North Dakota and hereby approved.

Grant McGimpsey
Dean of the School of Graduate Studies

November 28, 2018
Date

PERMISSION

Title   Comparing Source Rock Maturity with Pore Size Distribution and Fluid Saturation in the Bakken-Three Forks Petroleum System, Williston Basin, North Dakota

Department   Harold Hamm School of Geology and Geological Engineering

Degree   Master of Science

       In presenting this thesis in partial fulfillment of the requirements for a graduate degree from the University of North Dakota, I agree that the library of this University shall make it freely available for inspection. I further agree that permission for extensive copying for scholarly purposes may be granted by the professor who supervised my thesis work or, in his absence, by the chairperson of the department or the dean of the school of graduate Studies. It is understood that any copying or publication or other use of this thesis or part thereof for financial gain shall not be allowed without my written permission. It is also understood that due recognition shall be given to me and to the University of North Dakota in any scholarly use which may be made of any material in my thesis.

                                     Adedoyin Suleman Adeyilola
                                     December 13, 2018

TABLE OF CONTENTS

CHAPTER

LIST OF FIGURES

LIST OF TABLES

ACKNOWLEDGMENTS

To God Almighty

ABSTRACT

With the continuous demand for fossil fuel and advancement in technology, the unconventional petroleum resources have come into limelight. The Devonian Three Forks Formation consisting of carbonate and clastic sediments is an unconventional oil accumulation containing about 3.73 billion barrels of technically recoverable oil. However, understanding rock properties of the various lithofacies and fluid saturation is still challenging.

The petroleum prospectivity was evaluated by integrating organic maturity and hydrocarbon generation with porosity distribution and fluid saturation in the Ambrose field and adjacent fields. The organic maturity was done with a programmed pyrolysis analysis (Source Rock Analyzer) using samples taken at 1ft intervals through the Lower Bakken Shale. Core samples from the Lower Bakken Shale and Three Forks Formation were prepared for NMR analysis by saturating with 300,000 ppm NaCl brine solution at 100 psi of compressed air for 50 days. Porosity analysis was acquired from Helium porosimeter and quality checked by NMR transverse relaxation (T2) analysis with Oxford Instruments GeoSpec2 core analyzer coupled with Green Imaging Technology software. Pore size distributions were determined using T2 cutoff values to partition total porosity measurements into micropores, mesopores and macropores.

Tmax from the programmed pyrolysis showed that the organic maturity between wells varies from immature to mature (427°C to 440°C). NMR relaxation time results showed saturation is proportional to distribution of pore size with mesopore and macropore contributing more to oil saturation while micropore contributes to water saturation.

CHAPTER I

INTRODUCTION

The Williston Basin is an intracratonic sedimentary basin (Carlson and Anderson, 1965) spanning parts of Montana, South Dakota, North Dakota and Saskatchewan. The basin contain sediments that range from the Cambrian to tertiary age with the thickest part of the basin in western North Dakota. The Devonian and Mississippian Bakken-Three Forks petroleum system directly underlies the Madison Group and overlies the Bird Bear Formation. It is mainly an association of tight carbonates, clastic sediments and anhydrites.

The Bakken Formation is remarkable in the Williston basin due to the high source rock potential of its shale members (Dow 1974) and it is believed to source adjacent reservoir formations. The Bakken Formation consist of four (4) members (Meissner 1991) namely 1) the upper shale member 2) the middle siltstone/limestone/dolostone, 3) the lower shale member and the Pronghorn member. The Bakken-Three Forks system mainly unconventional (Lefever et al. 1991) and continuous petroleum accumulation (Nordeng et al. 2010). The amount of oil in place within the Bakken- Three Forks system is estimated to be about 7.8 billion barrels with almost a half of it from the Bakken Formation while the other half is from the Three Forks Formation (Gaswirth and Marra 2015). Apart from being a thermally matured and prolific a source rock, the Bakken Formation has produced an appreciable amount of oil through advanced drilling, completion and stimulation techniques (Lefever and Nordeng 2015). Oil discovery and production in the Bakken-Three Forks system began in 1953 from the Antelope with vertical wells (Nordeng and LeFever 2015).

Hypothesis

The occurrence of oil and gas in rock is influenced by the organic matter content and thermal maturity of the adjacent source rock. Hydrocarbon generated are not evenly distributed in the reservoir rock, instead, their proportions varies with pore sizes distribution. It is proposed that source rock in wells with higher thermal maturity should have the higher hydrocarbon saturation. If generated hydrocarbon migrates from the source rock to the reservoir, lithofacies with the highest porosity may not necessarily have the highest oil saturation because of pore sizes distribution.

Aims and Objective

To provide the thermal maturity of the Bakken Shale, porosity and saturation of oil in the Three Forks reservoir lithofacies, the following research objectives were met;

- Determining the geochemical properties of the Bakken Shale through pyrolysis
- Identifying and correlating reservoir lithofacies within the Three Forks Formation
- Estimating porosity and pore size distributions within reservoir lithofacies
- Compiling saturation data and distribution of pore fluids within the pores spaces.

Previous Work

Studies of the Bakken Formation date back to 1953 when it was first described by Nordquist (1953) for strata occurring between the depths of 2931 to 2963m in the Amerada H.O. Bakken #. Kume (1963) re-evaluated Norquist's Bakken Formation interval and came up with modified sample description. He re-estimated the thickness of all the members from core samples in the C. Dvorak #1 well, Dunn County, North Dakota. Fuller (1956) identified a basal conglomerate with erosional surface separating the Bakken formation from the underlying Three

Forks formation. Fuller (1956) suggested the black shales were deposited in a swamp that was formed due to the retreating Devonian seas. He therefore, attributed the Devonian age to the Bakken Formation based on lithology and paleontology data. Christopher (1961) identified the three (3) members of the Bakken to consist of similar upper and lower shale with a middle member sandstone. He distinguished individual members with contacts, identified erosional surface at the base of the lower Bakken member and a disconformity bounding the upper shale member. Hayes (1984) suggested an erosional surface occur between the Upper and Middle member of the Bakken based on difference in conodont fauna and assigned a Mississippian –Devonian age to the Bakken Formation.

The upper and lower Bakken Shales are organic rich and are regarded as a significant source rock for hydrocarbon generation in the Williston Basin. Webster (1984) described the Bakken Formation as a world class source rock with total organic carbon content averaging 11wt.%. The upper and lower Bakken shale members are sometimes characterized by anomalously high gamma-ray radioactivity, anomalously low but highly variable sonic velocity and resistivity (Meissner, 1991). Dow (1974) identified the Bakken Shale as the source rock for the Type II oil in the Madison reservoirs of Williston Basin. He argued that the Bakken shale has similar geochemical properties with the Madison oil. Williams (1974) used carbon-isotope ratios to classify the Bakken source rock as a Type II oil. He also analyzed 26 samples of Bakken shale and found them to contain from 0.65 to 10.33 wt.% organic carbon, with an average of 3.84 wt.%. Jin and Sonnenberg (2012) carried out a basin wide source rock analysis of the Bakken shale and identified a TOC range of 0.2 – 26 wt.% with an average of 20 wt.%.

The stratigraphy of the Bakken Formation includes three main members, the Upper and Lower shale members, and a middle mixed siliciclastic and carbonate member (Meissner 1978). Murray (1968) described the distinctive wireline signature of the Bakken Formation, subsequently, he ascribed source rock and reservoir properties to them. Fuller (1956), Christopher (1961) and Lefever et. al (1991) all described the stratigraphy of the Bakken Formation and interpreted depositional environment to range from marine swamp to deep offshore environment.

Peale (1893) first used the term "Three Forks Shale" for the argillaceous and calcareous beds outcropping between the Mississippian limestone and Devonian dolomitic limestone in Montana. Haynes (1916) used regional stratigraphy and paleontology to subdivide it into seven (7) units, thereby changing the name to Three Forks Formation. Christopher (1961) used the term Three Forks Group to include three formations in the ascending order, Torquay Formation, Big Valley Formation and Bakken Formation. The lithofacies and stratigraphy have been studied by Bottjer et al. (2011), Sonnenberg et. al (2011), Nordeng and LeFever, (2015), Nordeng et al, (2015) and (Sonnenberg 2017). They all identified three informal members with the main lithologies being mudstone, dolostone and anhydrite. Three Forks Formation is Devonian age (Christopher, 1961) and interpreted to be deposited in shallow marine to supratidal environments in a shallow epeiric sea (Dumonceaux, 1984). Garcia-Fresca et. al (2017) suggested a continental setting with little to no marine influence, in subaerial and subaqueous environments.

Bakken Petroleum System

The Bakken Petroleum system is an unconventional system (Meissner, 1991) with a continuous petroleum accumulation (Nordeng 2009). He described a continuous petroleum system as being independent of buoyancy, thus hydrocarbon generated from the source rocks are injected into the reservoir that includes the source rock and adjacent rocks (Figure 1). The upward migration

of hydrocarbon generated is hindered by the surface tension existing between the hydrocarbon and the water-saturated rocks. The Upper and Lower Bakken shales serve as source rocks while adjacent rocks around them such as Middle Bakken and Three Forks Formation serves as the reservoirs.

Nordeng (2009) continuous petroleum system is characterized by source rocks that are regionally extensive, organic rich and deeply buried to depths that are sufficient for hydrocarbon generation. The adjacent rocks above and below the source rock have sufficient permeability and porosity to contain hydrocarbon in commercial quantities. This entire system is confined by laterally extensive, thick and impermeable overlying and underlying rocks.
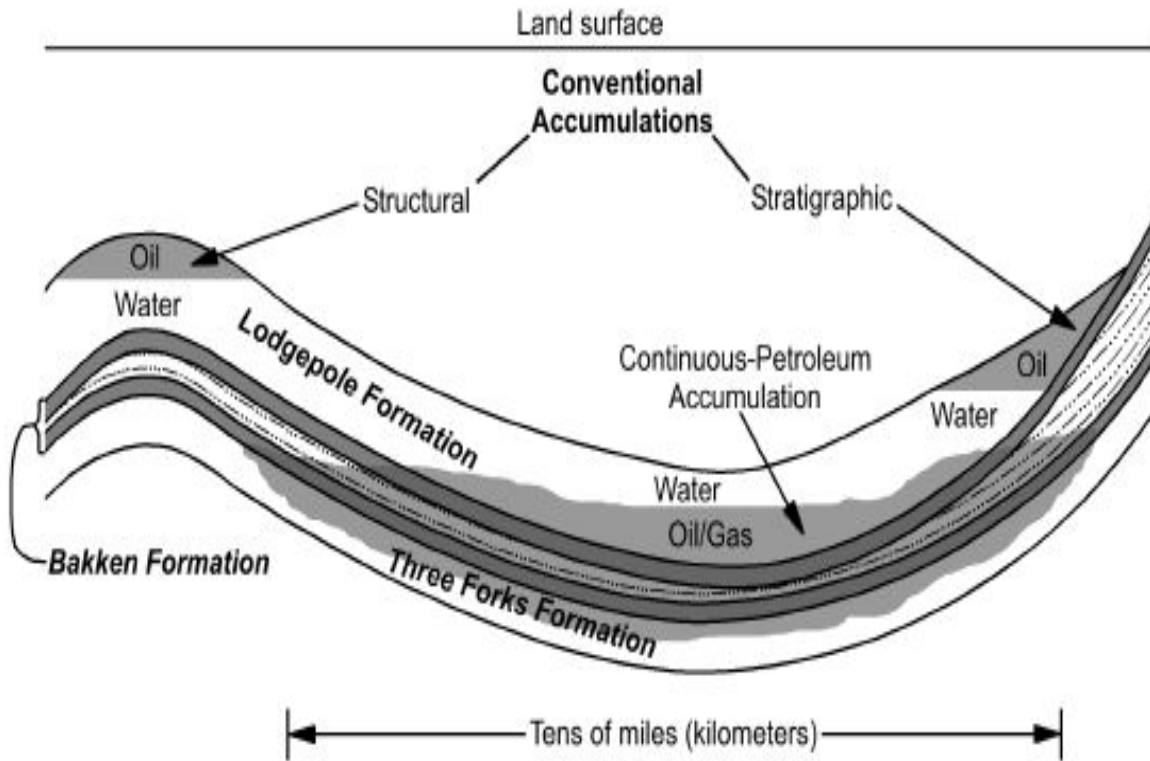
Figure 1. Schematic cross-section illustrating the continuous Bakken petroleum system (Nordeng 2009)

CHAPTER II

REGIONAL GEOLOGY

Early sedimentary processes, geographic distribution and facies association in the northern Great Plains reflects the tectonic history of the western border of the North American craton (Peterson and MacCary, 1987).

The main part of the Paleozoic craton consist of a stable core, the Transnational arch, the Canadian shield of older Precambrian rocks and its southwestern extension.(Figure 2). During the early to middle Paleozoic, the transcontinental arch divided the continent into eastern and western marine shelf and geosynclinal provinces, as approximate mirror images of each other. The Cordilleran shelf extends around the western part of the Paleozoic craton which is situated to the west of the Canadian shield and transcontinental arch. Here, the shelf harbors shallow marine sedimentary cycle during the early and mid-Phanerozoic. (Peterson and MacCary, 1987).

The western bound of the shelf was a gradually subsiding marginal basin with shallow water Paleozoic marine sediment accumulations extending through the southwestern United States to northwestern Canada. The combination of thrusting, mountain building and island growth in this western part facilitated the deposition of deepwater shales, fine grained limestone and submarine volcanic deposits in the Paleozoic. (Peterson and MacCary, 1987).

The eastern part of the Cordilleran shelf underlies the Northern Great Plains adjacent to the Transcontinental arch. In this region, the development of several paleostructural features attributed to the evolution of the Cordilleran shelf influenced the sedimentation processes to varying extents. The Williston basin which began subsiding during the late Cambrian/early Ordovician was the most significant structural element in the Northern Great plains. Other regional structural elements

includes the Central Montana trough, Alberta Shelf and the Wyoming Shelf. Local features include the Sweetgrass arch, Central Montana Uplift, Cedar Creek anticline and the Black Hills Uplift. (Peterson and MacCary, 1987).

The evolution of the basin is linked to a distinct area of increased subsidence during Middle Ordovician time (Sandberg, 1962; Carlson and Anderson, 1965; Gerhard et al., 1982). Major tectonic features around the Williston basin defines the boundaries (Figure 3). The northern part is bounded by Lower Paleozoic uplifts of the Meadow lake escarpment and the late Devonian Sweetgrass arch separating sediments of same age in the Alberta Basin lying northwest of Willison basin bounds the west. The south and southeastern flanks are bounded by the younger Tertiary Black Hills uplift and the older Silurian uplift of the Cedar creek anticline respectfully. (Gerhard et al., 1990).

Regional Sedimentology and Sequence

The sediments in the Williston basin were divided into continental-scale packages representing relative sea level rise, subsequent sedimentation, and then relative sea-level "drop" with accompanying disconformity (Gerhard 1990). The Lower Devonian to Mississippian sediments are classified as Kaskaskia sequence with their basal part defined by an unconformity overlying the Interlake Formation (Peterson et. al 1987). They are characterized by two regional sea-level rises and an unconformity that distinguish it from the upper Devonian and younger Kaskaskia sequence (Figure 4). This unconformity is significant not only in the Williston basin, but also in the entire western United States (Gerhard et al. 1990). The lower Kaskaskia sequence comprises those rocks overlying the Interlake or older formations and underlying the Bakken Formation. Subsequent rapid sea-level rise characterized the deposition of the Bakken Formation, the basal stratigraphic unit of the upper Kaskaskia (Gerhard et al. 1990).

Geology of the Bakken and Three Forks Formation

Bakken Formation

The Bakken Formation is Late Devonian to Early Mississippian age (Hayes 1984, Thrasher 1985 and Holland et al., 1987). It is uncomfortably overlain by the dark grey to brownish grey shale and limestone of the Mississippian Lodgepole formation (Webster, 1984). The thinly interbedded dolostone, siltstone and anhydrite of the Devonian Three Forks Formation uncomfortably underlies the Bakken Formation (Kume, 1963). The Devonian-Mississippian boundary is placed within the Bakken Formation in the Williston Basin (Peterson and MacCary, 1987). Bakken Formation has four (4) formal units within the Williston basin; the lower organic-rich black shale with minor siltstone, a middle dolomitic siltstone, an upper organic rich black shale and the intercalated pronghorn unit (Meissner, 1978). The thickness of the Bakken Formation varies within its depositional limits. It attains a maximum thickness of 145ft at its depocenter in the western Montrail County of North Dakota (Webster, 1984) and thins at its margin on the eastern, southern and southwestern flank (Meissner 1978)

The Lower and Upper Bakken Shale units consist of a dark-grey to black non-calcareous, fissile organic rich shale with more or less uniform lithology within its entire section in North Dakota (Lefever 1991 and Meissner 1978). The texture of the Lower Bakken shale can vary from finely laminated to massive (LeFever et. al. 1991) with a maximum thickness of 50 ft in the western Montrail County (Webster 1984). Hayes 1984 worked extensively on the biostratigraphy of the Bakken Formation. Among the fossils he identified in the lower Bakken shale are algae plant spores, conodonts, inarticulate brachiopods, fish teeth, bones and scales. The Lower Bakken Formation contains abundant pyrite and can be fractured in various orientations within the basin (Lefever et al .1991).
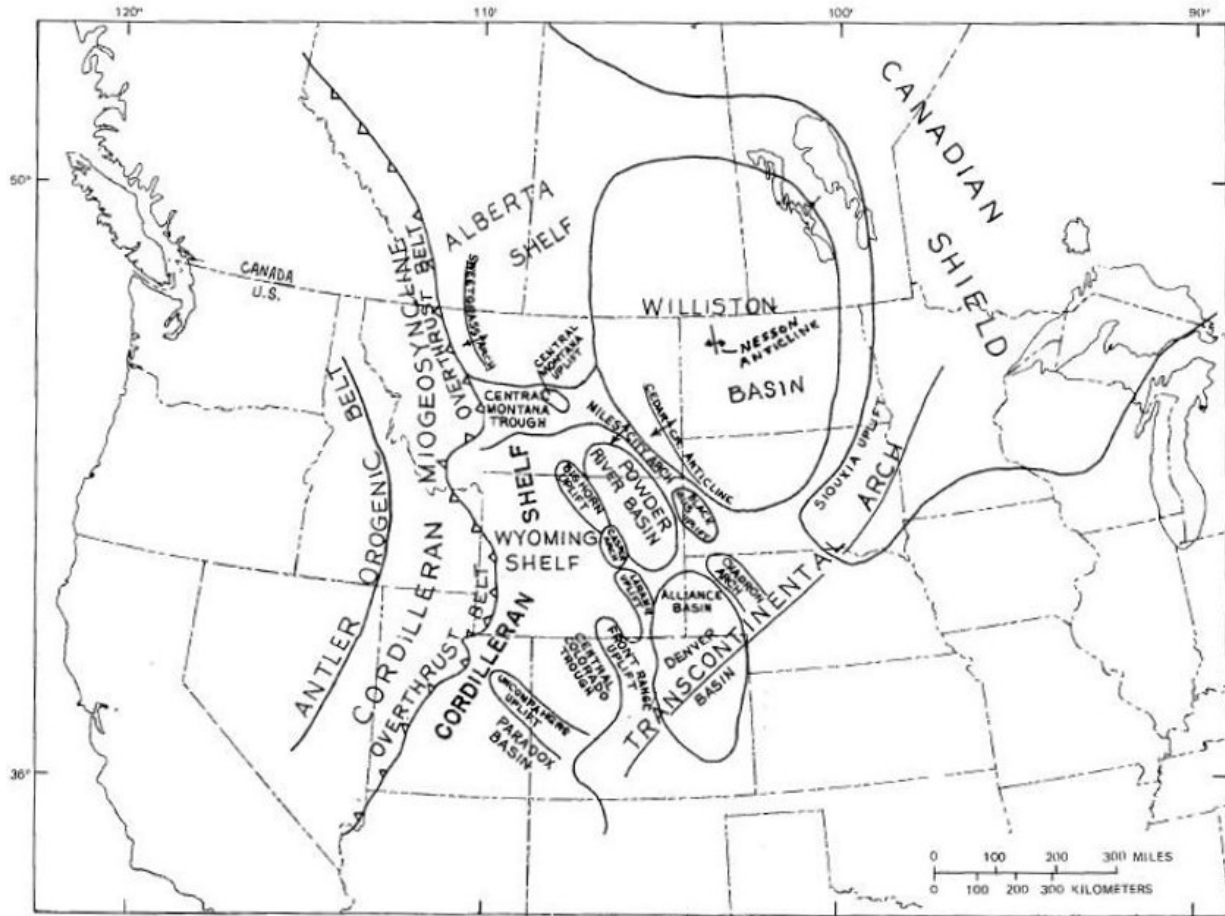
Figure 2. Regional paleogeography and paleostructure during Paleozoic and Mesozoic time Western Interior of United States (Peterson, 1981)
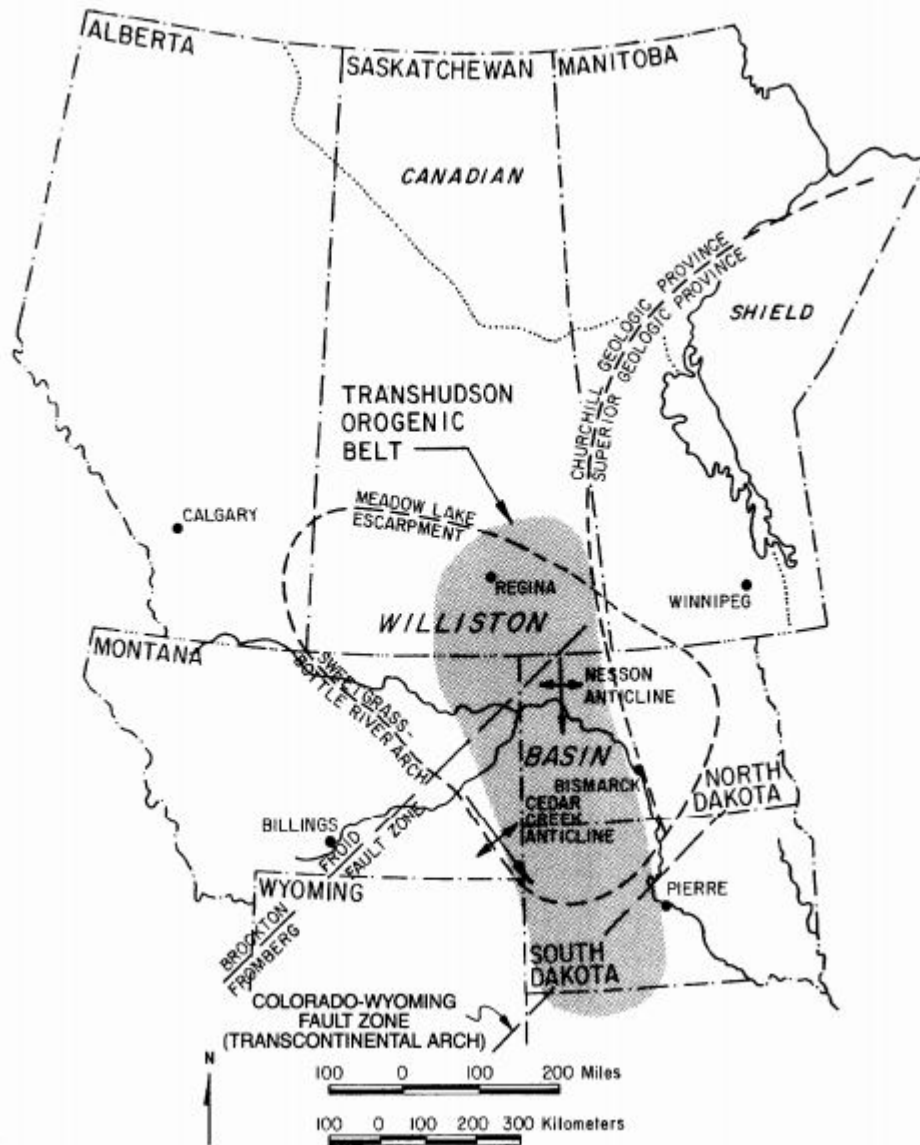
Figure 3. Location map of the Williston Basin and its bounding structural features (Gerhard et. al 1990

Left column:

SYSTEMS	TEJAS SEQUENCE	ROCK UNITS
QUATERNARY		PLEISTOCENE
		WHITE RIVER
TERTIARY		GOLDEN VALLEY
		FORT UNION GROUP
CRETACEOUS	ZUNI	HELL CREEK
		FOX HILLS
		PIERRE
		JUDITH RIVER
		EAGLE
		NIOBRARA
		CARLILE
		GREENHORN
		BELLE FOURCHE
		MOWRY
		NEWCASTLE
		SKULL CREEK
		INYAN KARA
JURASSIC		SWIFT
		RIERDON
		PIPER
TRIASSIC	UPPER ABSAROKA	SPEARFISH ● "unrestricted"
PERMIAN		

Right column:

SYSTEMS	SEQUENCE	ROCK UNITS
PERMIAN	UP ABSAROKA ABS.	MINNEKAHTA
		OPECHE
PENNSYLVANIAN	LOWER ABSAROKA	BROOM CREEK
		AMSDEN
		TYLER ●
MISSISSIPPIAN	UPPER KASKASKIA	OTTER
		KIBBEY ●
	MADISON	POPLAR INTERVAL
		RATCLIFFE INTERVAL ●
		FROBISHER ALIDA INTERVAL ●
		TILSTON INTERVAL ●
		BOTTINEAU INTERVAL ●
		BAKKEN ●
DEVONIAN (Upper Devonian)	LOWER KASKASKIA	THREE FORKS ●
		BIRDBEAR ●
		DUPEROW ●
		SOURIS RIVER
		DAWSON BAY ●
(Middle Devonian)		PRAIRIE
		WINNIPEGOSIS ●
		ASHERN
SILURIAN	TIPPECANOE	INTERLAKE ●
		STONEWALL ●
ORDOVICIAN		STONY MTN.
		RED RIVER ●☼
	SAUK	WINNIPEG GROUP ☼
CAMBRO-ORD.		DEADWOOD ●☼
PRECAMBRIAN		●

Figure 4. Generalized stratigraphy and sequences of the Williston Basin show the lithology and hydrocarbon types (Gerhard et. al 1990)

Legend

Oil ●
Gas ☼

12

The Middle Bakken unit is a mixed lithology. It consist of interbedded massive to cross-bedded siltstones and sandstones with dolomitized limestone (LeFever et. al .1991, Webster 1982, Hayes 1988, Thrasher 1985). Fossils identified within this unit includes articulate and inarticulate brachiopods, conodonts, plant spores, gastropods and various trace fossils (Hayes 1984). The maximum thickness of the Middle Bakken Formation in North Dakota is 87 ft in the eastern part of the Nesson anticline. The upper Bakken has a similar lithology and uniformity as the lower Bakken (Webster 1982, Hayes 1984) but differs with the absence of crystalline limestone, greenish shale beds and higher organic content with a maximum thickness of 28 ft. in North Dakota (Lefever et. al .1991).

A number of authors have worked on the depositional environment of the Bakken shales with various conclusion. Fuller 1956 and McCabe 1959 both suggested a marine swamp environment with restricted circulation as a result of abundant organic development for the shales. Christopher (1961, 1962) proposed a shallow marine environment with a restriction of free flow water. Webster (1984) proposed an offshore marine environment with anoxic conditions caused by stratified water column and restricted circulation. The Middle Bakken Formation is considered to be deposited during sea water incursion onto the land based on its overlapping stratigraphy with the lower Bakken Shale. (Webster 1982; 1984; Hesker and Smoker 1985)

The Bakken Formation is a superb source rock and was considered to be the source rock for most Mississippian reservoirs in the Williston Basin (Dow, 1974; Webster, 1984; Price et al., 1984). Jin and Sonnenberg (2012) found TOC content could range from 0.2 to 26 wt.% with an average of 20 wt.%. Williams (1974) used carbon-isotope ratios to correlate the origin of the Type II oils found in Mississipian rocks to the Bakken shales. Recent work has shown that the Lodgepole Formation was the source of at least some of the Mississippian oils (Osadetz and Snowdon, 1986).

Price and LeFever (1994) determined that the Bakken oils were confined to the Bakken source system (uppermost Three Forks Formation to lowermost Lodgepole Formation), and have not migrated into the overlying Mississippian reservoirs as previously thought.

The wireline response of the Bakken Formation have an unusually high Gamma Ray value greater than 200 AP and high interval transit time (80 -120 microsec/ft). (Meissner 1978, Webseter 1982 and 1984). Resistivity varies with maturation and depth with values greater than 100 ohms-meters below 8000 ft and less 100 ohm-meters above 7000 ft (Webster 1984).

Three Forks Formation

The Three Forks Formation is in Devonian age. It conformably overlies the Birdbear Formation (Devonian) and can be divided into three informal members, in ascending order: lower, middle, and upper (Bottjer et al, 2011; Nordeng and LeFever, 2015; Nordeng et al, 2015). The Three Forks Formation attains a maximum thickness of 270ft in the Dunn and eastern McKenzie counties (LeFever and Nordeng 2008).

The Three Forks Formation primarily consist of mudstone, dolostone and massive anhydrite at the low units. An informal unit, called the Sanish sandstone, can be developed at the top of the Three Forks Formation (Lefever and Nordeng 2009). The Three Forks Formation is interpreted to be deposited in shallow marine to supratidal environments in a shallow epeiric sea (Dumonceaux, 1984). Garcia-Fresca et. al (2017) used core, petrography, geochemical analyses, and isochore maps to propose to a continental setting with little to no marine influence, in subaerial and subaqueous environments. This is said to be comparable to those found in playa lake systems or continental sabkhas.

A total of 3.76 billion barrels of oil is estimated to be present in the Three Forks Formation with its sweet spots around regions where the Bakken shale has high thermal maturity (of the Bakken Formation (Gaswirth and Marra 2015).

A number of authors have worked on classifying the Three Forks Formation into different units and lithofacies. (Haynes, 1916) used fossils to subdivide the Three Forks Formation into seven (7) units. He identified the Yellow limestone, pale yellow shale, purple fissile shale, blue-gray nodular limestone, green shale, Yellow crystalline limestones and the yellow to orange black shales. Sloss and Laird (1947) researched the Logan section in the south central Montana and compared their findings with the work of Peale (1893) and Haynes (1916). His sub divisions were similar to those of Peale (1893) and Haynes (1893) but he identified the Jefferson Formation between the yellow limestone and yellow blocky shales.

Sanberg and Hammond (1958) classified the Three Forks Formation to include all strata below the Bakken Formation and above the BirdBear Formation. This interval was studied at the Mobil No.1 Birdbear well and consists of various lithologies including interbedded and interlaminated grayish-green and reddish brown micrite and dolomicrite.

Christopher (1961) defined the Three Forks group as the sets below the argillaceous Bakken Formation and above the dolomitic limestone of the Birdbear. These formations in the ascending order are Torquay, Big Valley and Bakken Formation. The Torquay Formation was further subdivided into six (6) units with the various units alternating between shale, dolomite, mudstone and anhydrite.

Dumonceaux (1984) subdivided the Three Forks Formation into five (5) lithofacies based on a comprehensive study that included core samples, petrographic and biostratigraphic analysis.

She identified micrite, argillaceous micrite, dolomicrite, argillaceous dolomicrite and argillaceous biomicrite lithofacies. Nordeng and LeFever (2009) subdivided the Three Forks formation into six (6) informal units based on lithofacies, sedimentary structures and wireline log signatures. Some of the surfaces and markers they used for their classifications were similar to Christopher (1961) markers. They observed the lower portions of the Three forks have abundant brecciated rocks and anhydrite nodules decreasing towards the upper strata. Above the "Unit 3", Nordeng and LeFever (2009) observed that primary sedimentary structures were more important in separating the various lithofacie into units.

Bottjer (2011) informally classified the Three Forks Formation into upper, middle and lower unit based on marker beds identified in the Birdbear well (Figure 5). The unit 6 of Christopher (1961) and Nordeng (2009) correlates with his Upper Three forks, units 4 and 5 correlates with the Middle Three Forks while the units 2 and 3 correlates with the lower Three Forks. He integrated stratigraphic surfaces, lithofacies and wireline signatures in making his subdivisions.

Western Canada (Christopher 1961; Smith and Bustin 2000)		North Dakota Dumonceaux (1984)		North Dakota Berwick (2008)			North Dakota Nordeng and LeFever (2009)		Bottjer et al.(2011); this study	
Torquay	Unit 6	Three Forks	Upper	Three Forks	Sanish	Facies E	Three Forks	Unit 6	Three Forks	Pronghorn
						Facies D				
						Facies C				Upper
	Unit 5					Facies B		Unit 5		
	Unit 4		Middle					Unit 4		Middle
	Unit 3							Unit 3		
	Unit 2		Lower					Unit 2		Lower
	Unit 1							Unit 1		

Figure 5. Correlation chart for the Three Forks Formation, Williston Basin, North Dakota, Montana, and Torquay Formation (Garcia-Fresca et al., 2017)

CHAPTER III

METHODOLOGY

Four wells (#22809, #28042, #23828 and #26745) from the Ambrose, West Ambrose and Colgan fields along the Divide County of North Dakota were used for this study (Figure 6). Divide County is situated at the northwestern edge of North Dakota, bounding Montana to the west, Saskatchewan to the north, Burke County to the east and Williams County to the south. All the wells are within a perimeter of 38 miles and an area of 82.5 mi^2 (Figure 7). Well log data were downloaded from the North Dakota Industrial Commission (NDIC) website and core samples were collected from the Wilson M. Liard core and sample library in Grand Forks. The list of wells used in this study is found in Table 1. The workflow for this study is listed below:

- Lithofacies identification and correlation

- Facie description

- Source rock analysis

- Porosity analysis

    - Sample preparation

    - Bulk Volume measurement

    - Helium porosity measurement

    - Sample saturation

    - Nuclear Magnetic Resonance (NMR) porosity measurement

Lithofacies Identification and Correlation

Physical core description and wireline logs wells were used to identify and correlate the source rock and the reservoir lithofacies (Figure 8). The Lower Bakken Shale was identified as the

source rock alongside seven (7) reservoir lithofacies within the Three Forks Formation. They are: 1) grey – tan laminated mudstone and dolostone; 2) tan massive dolostone; 3) tan - dark brown mottled dolostone; 4) green – grey massive mudstone; 5) grey and tan mottled mudstone; 6) grey and tan mudstone conglomerate; and 7) grey and tan brecciated mudstone.

Facies Description

1) Lower Bakken Shale: The color range from dark grey to brownish-black to black. Their grain size are fine and consist of clay minerals. Texture is massive with slight lamination. Contains some traces of limestone with dull yellow fluorescence. They are organically rich and contain pyrite nodules (Figure 9).

2) Laminated Lithofacies: It consists of finely interlaminated grayish-green to greenish-gray dolomitic mudstones and pinkish-tan silty dolostones. The laminations are flaser to wavy. Laminar bedding ranges from less than one cm up to approximately 15 cm with no preference to mineralogy. Unidirectional and bidirectional ripples are more pronounced in the tan dolostone compared to the green mudstone. Pyrite clusters and rip-up clasts of dolostones are also present. Lithofacies thickness is about 2 to 5ft (Figure 10).

3) Massive Dolostone: This a tan dolostone lithofacies which is mainly composed of silt and sandsize dolomite. The predominant grain size is silt (~0.04 mm), with some grains in the very fine sand range (~0.07 mm). It is composed mainly of dolomite and trace amount of quartz and clay. They also have subrounded lenses that are probable deformed dolomite-filled burrows. No major sedimentary structure, they have massive texture and scoured surfaces. Lithofacies thickness varies from 1 to 3ft (Figure 11).

4) Mottled Dolostone: Predominantly tan dolostone with interbed of green - grey mudstone. They contain about 20 to 40 percent thinly interbedded green mudstone that are highly folded and

deformed due to the soft sediment deformation. They are flaser bedded and slightly laminated. They also contain deformed thinly laminated silty dolostones. The predominant grain size is silt (~0.04 mm), with some grains in the fine sand range (~0.07 mm). Thickness of this lithofacies is approximately 1 to 4ft (Figure 12).

5) Massive Mudstone: This unit is a thinly laminated green to grayish-green mudstone. They are clay-sized, matrix supported rock with sparsely scattered, silt-sized, dolomite and quartz grains. Abundant pyrite crystals and crystal aggregates of variable sizes are distributed irregularly throughout this unit. The texture is massive with no visible sedimentary structure. Thickness of this lithofacies is approximately 0.5 to 3.5 ft (Figure 13).

6) Mottled Mudstone: It composed of light brown dolomitic shaly siltstone and gray to dark green dolomitic claystone. They are massive, slightly laminated, flaser bedded with irregular distribution of dolostones. Thickness range from less than 1 to 5ft (Figure 14). Slightly brecciated and chaotic. The predominant grain size is silt (~0.04 mm), with some grains in the fine sand range (~0.07 mm).

7) Mudstone conglomerates: This facies consists of green-grey dolomitic mudstone matrix with tan dolomitic clast. The clasts range in size from 0.5 to 2 cm and the matrix are predominantly silt size (~0.04 mm). Moderate to well-rounded and poorly sorted. Brown in the deeper section of Middle Three Forks due to oxidation. The system is matrix supported with visible sedimentary structure (Figure 15).

8) Brecciated Mudstone: Composed of brecciated layers interbedded with reddish massive dolomitic mudstone with clasts. The clast are angular and poorly sorted. They are chaotic with no visible sedimentary structure. It is matrix supported at the top and clast supported at the base. The matrix is silt size (~0.04 mm) while the clast range from <1cm to 3.5cm (Figure 16).
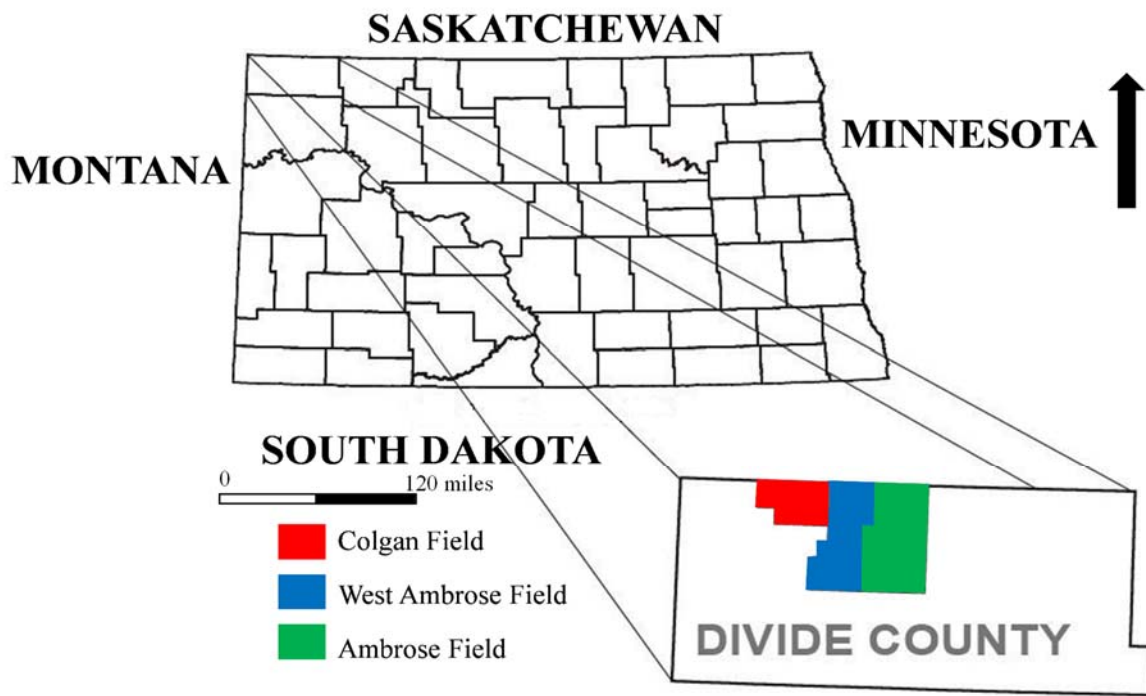
Figure 6. County Map of North Dakota showing boundary states. (Inset: Fields of interest in Divide county)
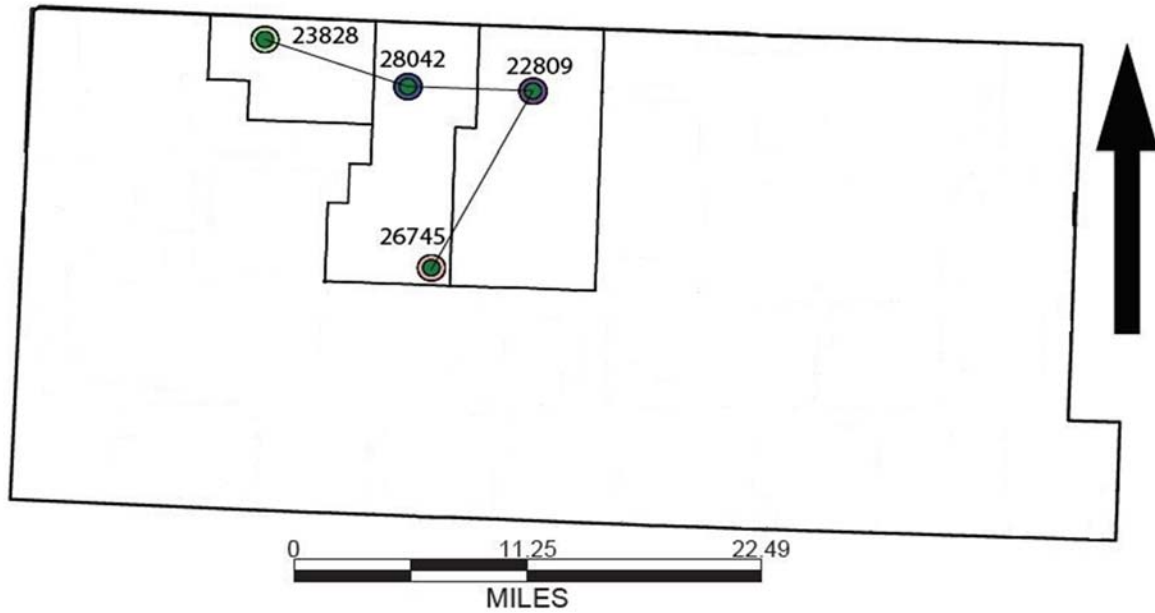
Figure 7. Study wells distribution in the Divide County

Table 1. List of lithofacies and their corresponding depth in the study wells.

Well Name	BAJA 1522-04TFH	TOMLINSON 3-1HN	TORGESON 2-15HS	MUZZY 15-33S-164-101
NDIC Number	#22809	#26745	#28042	#23828
	Depth (ft)	Depth (ft)	Depth (ft)	Depth (ft)
Shale	7955	8708	7970	7941
Laminated	8033	8765.5	8023.7	7986
Massive dolostone	7993	8728.6	7981	7949
Mottled dolostone	7990	8749.5	7988	7980.2
Massive mudstone	7998	8736.2	8000.1	7957
Mottled mudstone	8024.3	8762	8014.5	7978
Mudstone conglomerates	8006	8739	8005	7963
Brecciated mudstone	8030	8778	8037	7999.2
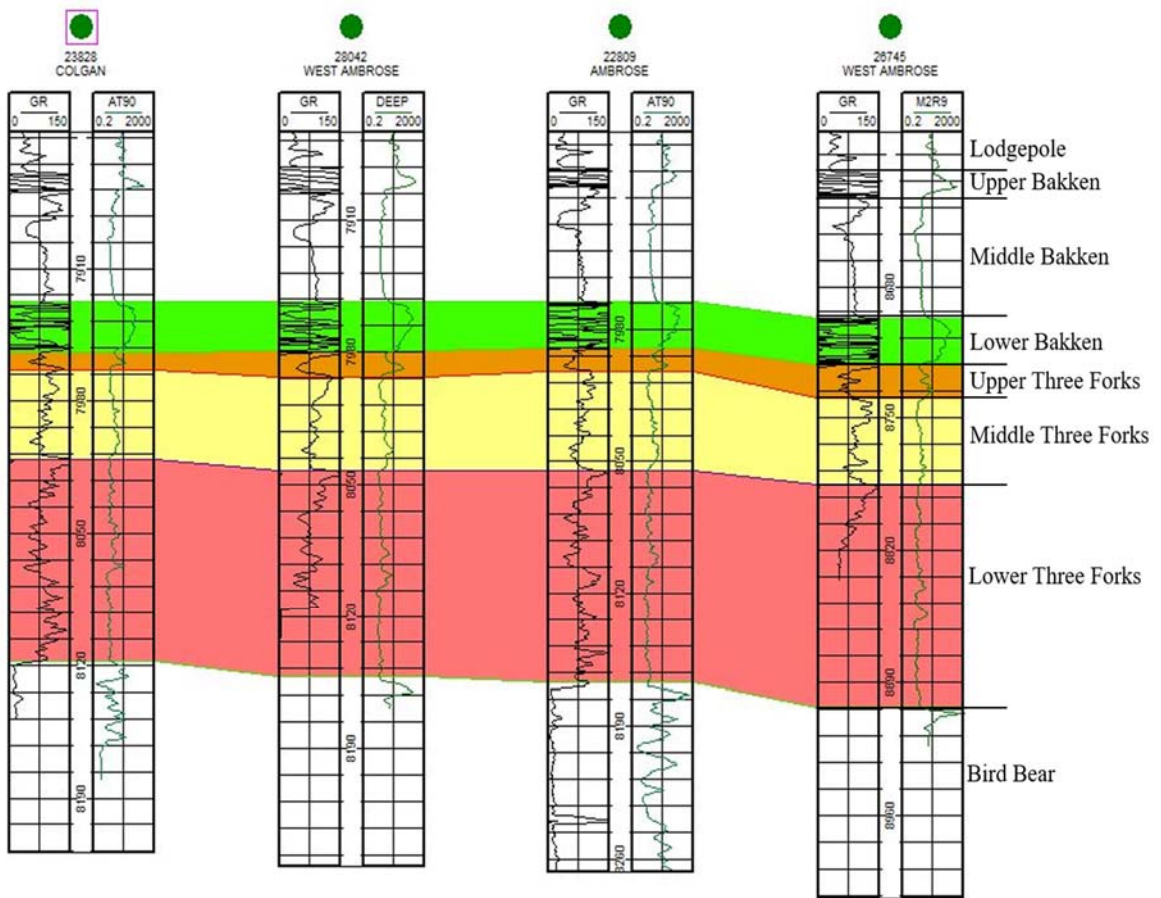
Figure 8. Lithostratigraphic correlation within the Lower Bakken and Three Forks in the study wells.

Figure 9. Lower Bakken Shale
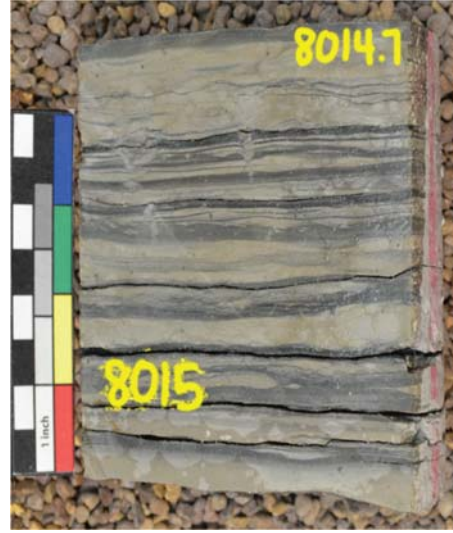
Figure 10. Laminated lithofacies

Figure 11. Massive Dolostone

Figure 12. Mottled Dolostone

Figure 13. Massive mudstone

Figure 14. Mottled mudstone

Figure 15. Mudstone conglomerate
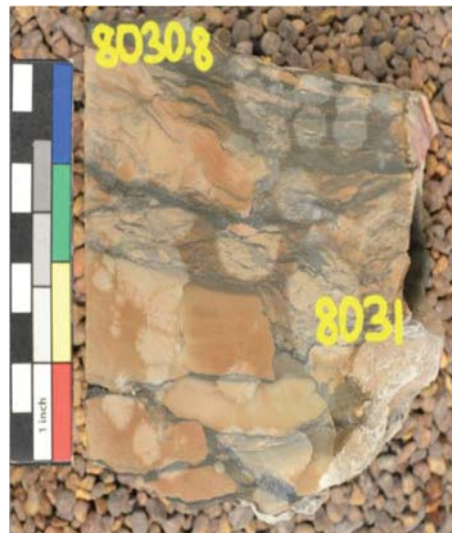
Figure 16. Brecciated mudstone

Source Rock Analysis

Rock-Eval pyrolysis is used to evaluate the petroleum-generative potential and thermal maturity of rocks. It is defined as the heating of organic matter in the absence of oxygen to yield organic compounds (Peters 1986). Espitalie et al 1977, worked on Rock Eval pyrolysis of whole rock samples, and the results were interpreted to provide information on the quantity, type and maturity of organic matter. Operating parameters for programmed Rock-Eval pyrolysis involves heating 60-80 mg of pulverized samples in at 300°C for 3 minutes, followed by programmed pyrolysis at 25°C/min to 650°C, both in a helium atmosphere (leckientz et. al 1979).

A flame ionization detector (FID) detects hydrocarbon compounds generated during pyrolysis. The first peak (S1) represents the milligram of free hydrocarbons that is liberated from the rock sample without cracking the kerogen during the first stage of heating at 300° C (Figure 17). The second peak (S2) represents the milligram of hydrocarbons generated by pyrolytic degradation of the kerogen in the rock at temperature between 300-650° C. The third peak (S3) represents the milligram of carbon dioxide generated from the rock during pyrolysis up to 390°C (Peters 1986). A thermocouple installed immediately below the sample measures the temperature during pyrolysis. The temperature at which the maximum amount of S2 hydrocarbons is generated is called Tmax. Tmax is a major index of maturity and as a rule of thumb, a range from about 435°C - 455°C implies maturity in most kerogen samples (Tissot and Welte, 1984).

The hydrogen index (HI) is the quantity of pyrolyzable hydrocarbon from S2 relative to the total organic carbon in the sample (S2/TOC). HI typically ranges from ~100 to 600 in geological samples, and a high value indicates greater potential to generate oil. HI can also be utilized to infer kerogen types. The oxygen index (OI) is the quantity of carbon dioxide from S3 relative to the TOC (S3/TOC). OI are used to track kerogen maturation and type. The production

index (PI) is the relationship between the hydrocarbons generated during the first and second stage of pyrolysis. It is expressed as the ratio (Sl/Sl+S2). PI is used to characterize the evolution level of organic matter, and it can be used as an indication for maturation. The S2/S3 values indicate the type of organic matter for low to moderately mature samples (Leckie et al 1988).

Procedure

About 60 – 80 mg of pulverized samples from each foot within the Lower Bakken Shale from all wells were transferred into the crucibles in the UND-Weatherford Source Rock Analyzer. The first crucible in the sequence is blank, this is done to allow the machine to perform a blank correction for all the subsequent samples in the crucibles. The analysis involves loading of a standard sample at every five (5) samples, to allow quality assurance and quality of results.
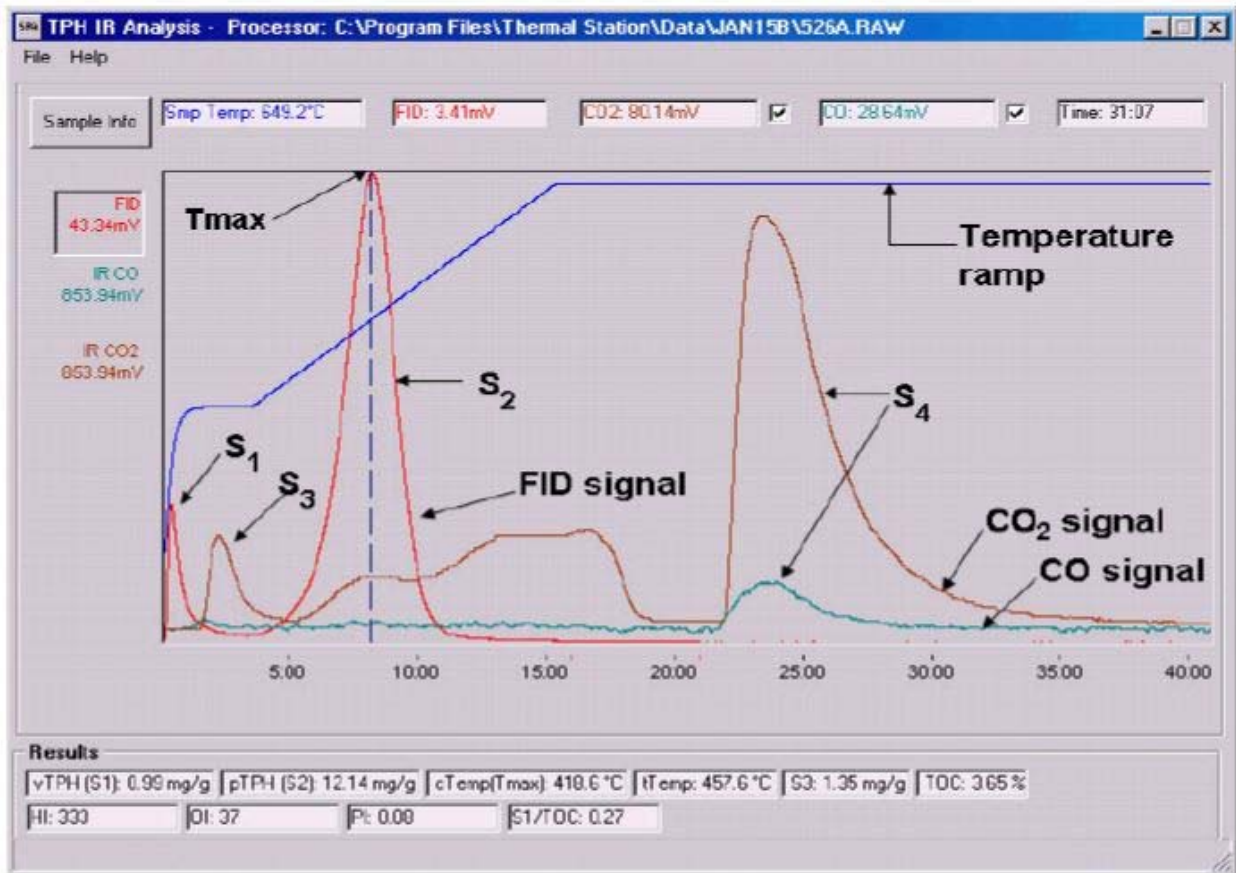
Figure 17. Plot of detected signal showing evolution of organic compounds from rock sample during heating with increasing time from left to right.

Porosity Analysis

The Helium porosimetry and nuclear magnetic resonance (NMR) methods were used to determine porosity in the lithofacies. The workflow for these analyses are in the order below:

- Sample preparation

- Bulk Volume measurement

- Helium porosity measurement

- Sample saturation

- Nuclear Magnetic Resonance (NMR) porosity measurement

Sample Preparation

All lithofacies were weighed and heated at 100 ⁰C in an isolated oven for seventy-two (72) hours, after which they were brought out and reweighed. A large decrease in weight was observed due to the heating and loss of fluids, they were subsequently placed in the oven at same temperature and weighed every twenty-four (24) until there was no changes in the weight. At this point, we were sure that the moist trapped within the samples were all evaporated. This methodology was adopted from Peterson (2017) sample preparation.

Bulk Volume Measurement

The mass and bulk volume of each lithofacies is a prerequisite for the helium porosimetry and NMR measurements. The helium porosimeter equipment is calibrated to use the measured bulk volumes with the grain volume and masses to estimate absolute porosity. All the core samples analyzed have irregular shapes, thus estimating their surface area and bulk volume manually with regular shape equations will either underestimate or overestimate the values. A NEXTENGINE 3D laser scanner was used to acquire the image of the lithofacies and processed with a ScanStudio software installed on a windows 10 computer system. The scanner emits beam and sends to the

sample, which is placed on a detached stage at a distance of 20-25cm from the scanner. The beam is reflected back by the sample and detected by a sensor that is housed within the scanner. The object is held in place on the stage by a set of three to six metallic stands while the stage is rotating at a fixed angle. Scanning is achieved by a combination of rotary movement of the object on the stage in the x, y and z directions and vertical movement of the sensor. A better scan is achieved when the samples have less angles and large exposure to the beam. Concave surfaces and surfaces oriented at a low angle ($< 20°$) to the beam will not produce a significant reflection. This method is fast, automated, accurate and non-destructive.

Procedure

Samples were placed at the center of the rotating stage and held firmly by the metallic stands to prevent shaking or any form of movement while rotating the axes. All the scans from each angle of rotation were represented by meshes and integrated together to form a full representation of the object. The aggregated meshes contains various edges, artifacts and scans of the metallic stands holding the samples on the stage. These unwanted scans were deleted, from the main aggregates, and then the entire volume is aligned, polished and solidified with the ScanStudio software. The surface area and bulk volume of the final solidified scan is estimated with the same software.

<div align="center">

Helium Porosity Measurement

</div>

The helium porosimetry method was utilized to measure porosity in all lithofacies. The porosity values from this analysis is used to check the level of precision with the porosity measurement from NMR analysis. Helium porosimeter works with Boyle's law

technique. The equipment consists of two sample chambers that are used to calibrate volume of samples. The calibration process involves injecting helium into the chambers and recording the pressure differences when the valve between the two chambers is open and equalization occurs. Upon calibration of sample volume, the sample is placed in one chamber at some pressure, p1, which is isolated from the second chamber at P_2. When the valve is opened, pressure equilibrium occurs at some final pressure, P_f. The pore space of the sample is penetrated by the gas; therefore, the gas volume difference between the two tests is a measure of the grain volume. The relationship between grain volume and bulk volume gives the porosity.

$$\Phi = 1 - \frac{Vgrain}{Vbulk}$$

Where V_{grain} and V_{bulk} are grain volume and bulk volume respectively

Procedure

A pre-calibrated Metarock PDP-300 Helium porosimeter was used to measure the porosity of rock samples. Bulk volume of core samples was obtained with 3D laser scanner. Core samples of known mass and bulk volumes were inserted into the matrix cup and filled with disks of known properties to make the core flush with the top of the matrix cup. The cup is inserted into the core holder that is attached to the porosimeter and tightened. The instrument mechanism allows high confining pressure from helium gas penetrate the pores within the core samples. The porosity is found by observing the change in pressure once the Helium gas is expanded, after it was pressurized into the sample.

<div align="center">

Sample Saturation

</div>

The NMR porosity acquisition requires samples to be partially or fully saturated with water or hydrocarbon. This is done because the relaxation time distribution in saturated rocks represents the pore-size distribution and porosity of the rock (Coates et al 1999). The laboratory procedure

involved transferring all the core samples into container in an evacuation flask that is equipped with vacuum source for 48 hours. The vacuum has a negative pressure of 50 psi that helps evacuation of air and vapor present in the pore spaces. 300,000 ppm of brine was gently introduced into the container in the evacuation flask with the water line being approximately 4 inches above the core samples. The choice of brine as the saturating fluid is to minimize salt dissolution since salts crystals are seen all over the Three Forks Cores.

The brine filled sample container were taken out of the evacuation flask and transferred into a pressurized chamber for 50 days to enable adequate saturation for NMR analysis. The pressure within the chamber were maintained between 100 and 120 psi. Paterson (2017) worked on the saturation of various Three Forks facies and observed a saturation of 81-95% at 100 psi after 25 days, therefore 50 days were suggested for this study.

Nuclear Magnetic Resonance

NMR measures the magnetization decay that results from the absorption and emission, of electromagnetic radiation by nuclei that possess a spin property when placed in a magnetic field (Abragam 1961). A permanent magnet and a radiofrequency pulse were deployed to measure the nuclear response to the permanent magnet (B_0) exposure (Figure 18). The magnet aligns the nuclei in a specific orientation, in a process called polarization. An intense but temporary oscillatory field is applied to tip the protons 90° to a new equilibrium position that is perpendicular to the direction of B_0. The removal of the oscillatory field causes the nucleus to return to the initial equilibrium state aligned with B_0.

Abragam (1961) describe the movement as Free Induction Decay (FID) and contains information on the hydrogen nuclei content and fluid contained in a sample. The time required for the nuclei to release its energy is called relaxation time. The relaxations time (T_1 and T_2) are signal decay times related to the various interaction of fluids with themselves, with solids, pore size and the magnetic pulse sequence used (Abragam 1961). They are controlled by the surrounding media and energy transfer (Moss et. al 2003).

Longitudinal relaxation (T_1) is the time needed to repolarize after a nuclear spin disturbance. This happens when an excited nucleus returns to it low energy state when it loses all its energy to the surrounding nuclei after a 90° pulse (Ashqar 2017). (Figure 19). Transverse relaxation (T_2) is the time taken for the nuclear spins to diphase after the static magnetic field B_0 is turned off in the transverse plane. T_2 occurs when the nucleus exchanges energy but does not lose it to the surrounding (Ashqar 2017).

Both relaxations T_1 and T_2 have similar distribution in porous rocks. Their value is influenced by the rock and pore space properties. T_2 value, however, is controlled by molecular interactions and the variations in static magnetic field. Therefore, T_2 is more often used than T_1 to determine the different reservoir properties (Coates et al 1999). T_2 values are always equal to or less than T_1 (Akkurt et al. 1996). Surface relaxation (T_S) also affects both T_1 and T_2. This type of relaxation arises when interaction between the fluid and the solid surface occurs due to the magnetic susceptibility contrast between grains and pore fluid (Korringa et al 1962).

The surface relaxation rate is given by:

$$1/T_S = \rho(S/V)$$

where ρ is the surface relaxivity and S/V is the pore surfaceto-pore volume ratio.
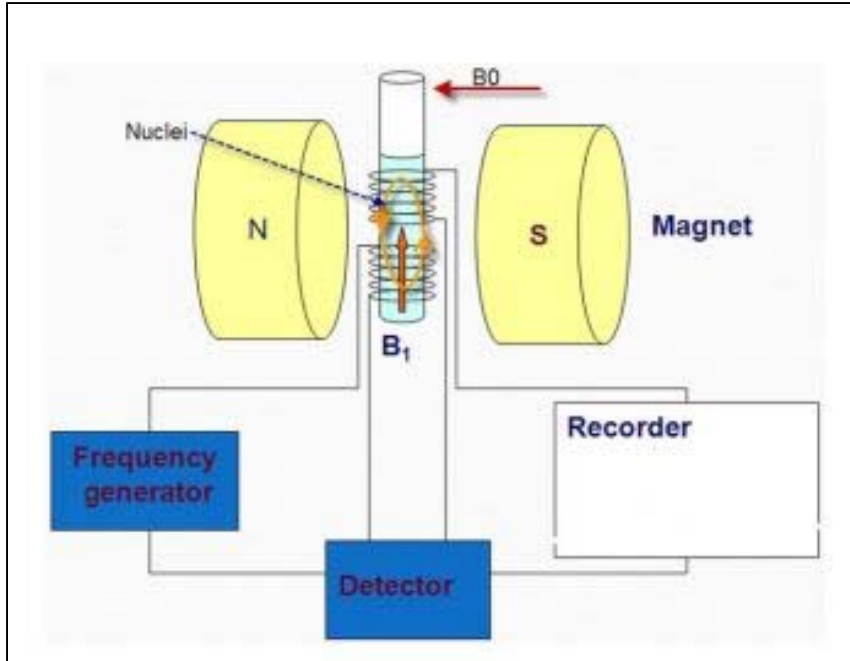
Figure 18. Diagrammatic representation of an NMR equipment showing the sample position, permanent and temporary magnets, and various instrument parts (Ashqar 2017)
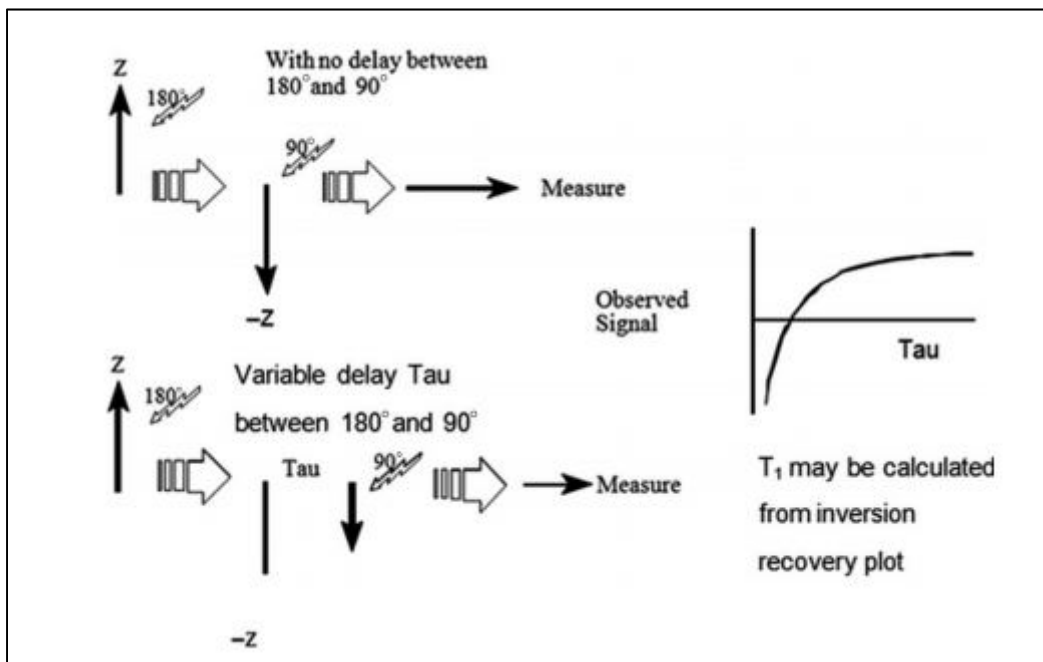
Figure 19. T1 detection and measurement principle, illustrating the different steps the nuclei goes through (Ashqar 2017)
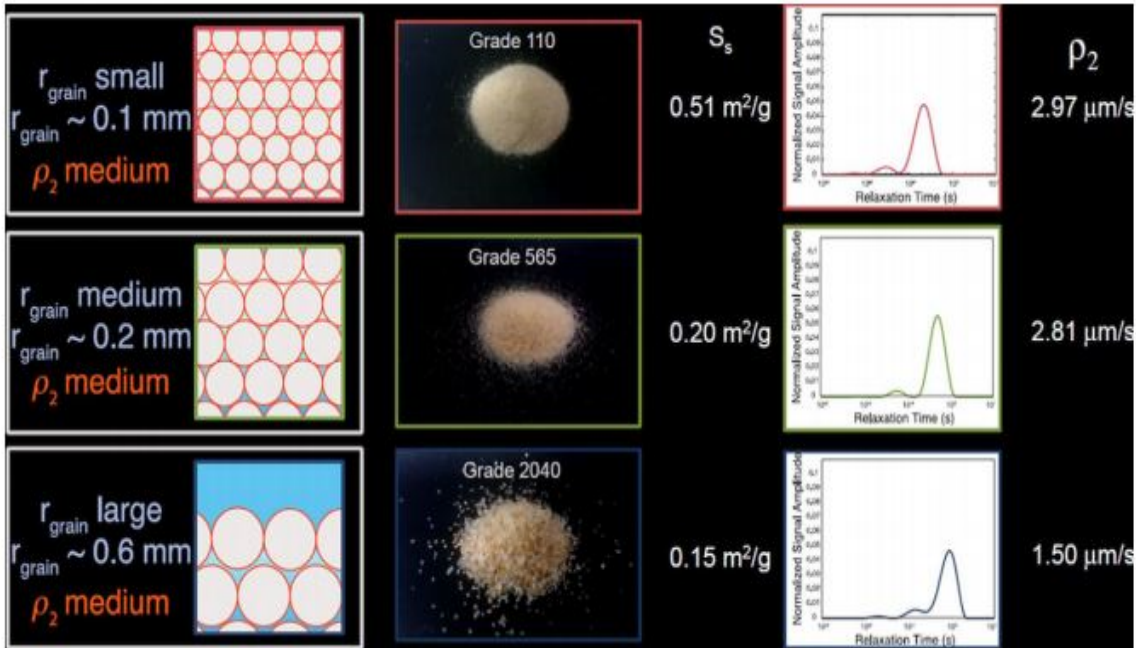
Figure 20. The relationship between surface relaxivity, grain radius and pore surface for sandstone. The Figure shows that a change in the grain size for the same type of rock leads to a change in surface relaxivity (Keating 2013).
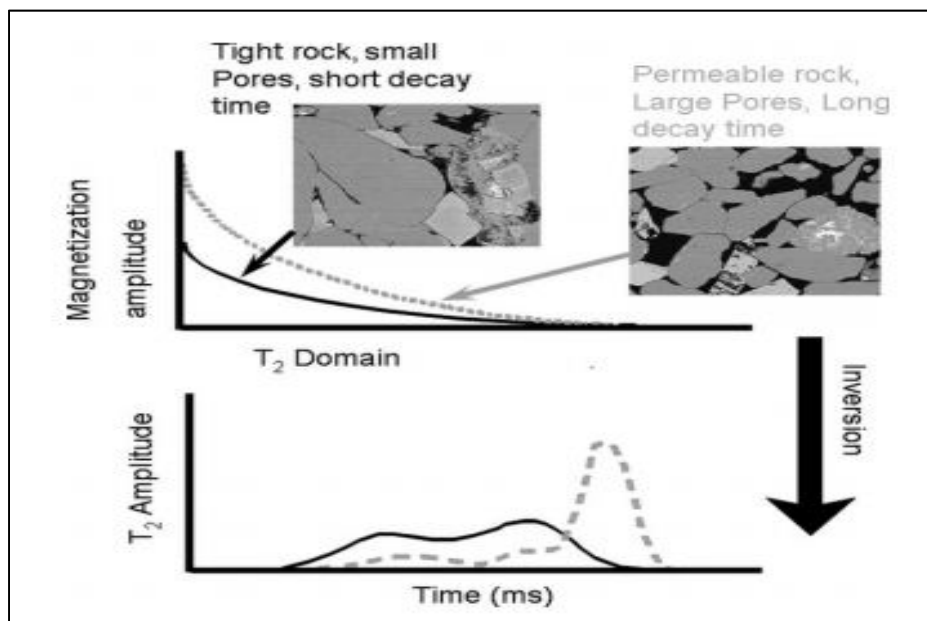
Figure 21. Surface relaxation mechanism and pore size effect; the upper section shows the relaxation mechanism and its realization when converted to pore size distribution according to pore size properties (Moss and Jing 2001)

Rock properties are a major influence on surface relaxivities, therefore a change in grain diameter leads to a change in the specific surface area, and consequently, surface relaxivity will differ (Ashqar 2017). As a result, an increase in surface relaxivity is related to a reduction in the grain size (Figure 20).

The relationship between pore sizes and surface relaxivity in rocks is inverse. Therefore, the larger the pores, the slower the relaxation time (Figure 21). The variation in pore sizes in any formation imposes different relaxation times, with each pore having a different relaxation T_2 value (Moss and Jing 2001)

The various fluid types (oil, gas, and water) and their distributions (moveable and nonmovable) within the pore space can be reflected in the overall NMR response. NMR can differentiate clay-bound from capillary-bound and movable water because each phase is located in a different portion of the pore space (Basan 2010). Allen et al., (2000) argued that the NMR decay spectrum can be divided into three divisions using the T_2 cutoff time of 3 and 33ms. Free fluid (T_2 values > 33 ms) are contained in larger pores with slowest T_2 time, capillary-bound water ($3ms < T_2 < 33ms$) are contained in smaller pores and faster T_2 time and clay bound water ($T_2 <$ 3ms) are contained in the smallest pore spaces with fastest T_2 time. The different cutoffs, mainly, divide the T_2 distribution into producible and irreducible porosity. The producible contains fluid that resides in the large pore bodies, while irreducible or bound fluid resides in the smaller pores. The sum of the two porosities is the NMR measured porosity, which can be written as follows:

$$\Phi = FFI + BVI$$

Where FFI is the free fluid index and BVI is bulk volume index.

FFI and BVI are the NMR-derived fractional volumes of free and bound fluid (Figure 22). The bulk volume index is characterized with short relaxations and slow diffusion as a result of nuclei movement restrictions in small pores.

Procedure

Upon saturation of samples, they were analyzed for total porosity and pore sizes distribution using the NMR T_2 relaxation time distribution with an Oxford Instruments Geospec 2 core analyzer. Each lithofacie from all the studied wells was inserted into the equipment sample hollow, which only take samples between the range of ½" to 6" diameter. The resonance frequency of the machine is calibrated at 2.4z MHz with a τ of 56 µs. The τ is the time between the 90° and 180° pulse in a spin echo train. The equipment was set to achieve a minimum signal to noise ratio (SNR) of 100 and maximum T_2 relation time of 100 ms for all samples. The results were displayed and interpreted with the Green Imaging Technologies software.
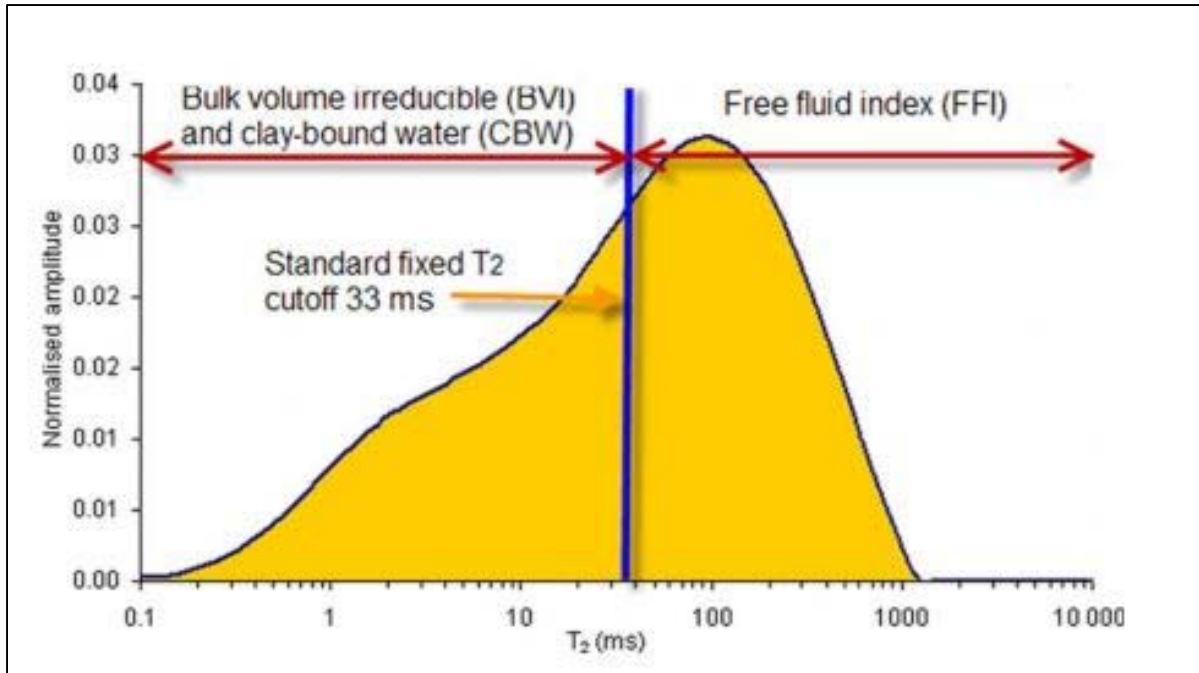
Figure 22. NMR T2 distribution showing the partition between BVI and FFI, modified from Coates et al.1999

CHAPTER IV

RESULTS AND DISCUSSIONS

Source Rock Results

The Rock Eval techniques were used to evaluate and compare the qualities and properties of the Bakken source rock in the studied wells. This method involves integrating the components of the source rock such as quantity of organic matter, types of organic matter, generative potential and thermal maturity. Tables 2, 3, 4, and 5 show the results of the source rock pyrolysis using wells 22809, 26745, 28042 and 23828 respectively.

Quantity of organic matter

The total organic carbon (TOC) and fraction of TOC that generated hydrocarbon during pyrolysis are significant in assessing the organic richness of a petroleum source rock. The TOC is the mass of carbon per unit mass of the whole rock. It is determined by summing the carbon in the pyrolyzate (S1, S2 and S3) with the carbon obtained by oxidizing the residual organic matter after heating to 650 °C (Peters, 1986). Therefore, TOC is greater than the cumulative carbon from S1, S2 and S3. Peter 1986 and Peter & Cassa 1994 classified the organic richness of a source rock with TOC and S2 values. The TOC and S2 values from the pyrolysis results were plotted for all wells to determine the level organic richness and quantity in Figure 23. The data showed that TOC in well 22809 range from 10.67 wt.% to 18.23wt% with an average of 14.26 wt.%, well 23828 has a range of 6.90wt.% to 18.83wt.% with an average of 13.63wt.%. Also, well 26745 has a TOC range of 9.81 wt.% to 22.19 wt.% with an average of 15.73 wt.% while well 28042 has a range of 5.35wt.% to 23.24wt.% with an average of 15.28 wt.%. All the data points plotted in the excellent TOC and S2 zone, with wells 28042 and 23828 having the widest distribution of data. Wells 22809 and 26745 have data points clustered within the excellent zone are excellent source rocks all in

terms of quality and quantity of organic carbon. In general, all the studied wells have excellent

richness and quantities of organic matter but in varying capacities.

Types of Organic Matter

The type of organic matter contained in a source rock is significant in predicting the

hydrocarbon generating potential of the source rock. Tissot et. al (1974) and Espitalide et al. (1977)

used pyrolysis indices to characterize kerogen types because they are independent of the

abundance of organic matter and are strongly related to the elemental composition of kerogen.

They classified kerogen types with a modified Van Krevelen diagram by replacing H/C with HI

and O/C with OI data from the pyrolysis. On the modified diagram, Type I kerogens are

characterized with high HI and low OI, Type III kerogens have low HI and high OI, and Type II

kerogen are intermediate. All the data points in the studied wells plotted within the type II zone on

the Van Krevelen diagram (Figure 24). This result is in conformity with the finding of previous

research by Dow (1974) and Williams (1974) for the Lower Bakken Shale. Waples (1985) also

classified the organic matter contained in the source rock into different types based on the

hydrogen index (HI) values. HI values < 150mg/g are classified as gas potential source rocks

(kerogen type III), 150 – 300 mg/g as oil and gas bearing with greater potential to generate gas

than oil (type II and III). HI values > 300 mg/g are largely type II and have higher potential for

generating oil than gas, while HI > 600mg/g consist mostly of type I and a II with excellent oil

generating potentials. The HI range in all the well samples range from 401 – 595 mg/g, they are

all within the range > 300 mg/g and less 600mg/g. This is the zone of type II with high oil

generating potential.

Table 2. Rock–Eval pyrolysis result for well 22809

						WELL #22809							
						Member: Lower Bakken Shale							
Sample	Depth	TOC	S1	S2	S3	Tmax	Calc.	HI	OI	S2/S3	S1/TOC * 100	PI	S1+S2
# ID	(ft)	wt%	mg HC/ g rock	mg HC/ g rock	Mg CO2 /g rock	(°C)	% Ro	Mg HC /g TOC	MgCO2 /g TOC				
22809-1	7959	13.77	3.58	74.02	0.70	435	0.68	538	5.1	105.74	26.00	0.05	77.60
22809-2	7960	14.24	3.49	73.09	0.33	435	0.67	513	2.3	221.48	24.51	0.05	76.58
22809-3	7961	17.87	6.05	92.84	0.43	434	0.65	520	2.4	215.91	33.86	0.06	98.89
22809-4	7962	16.80	6.46	87.61	0.48	436	0.69	521	2.9	182.52	38.45	0.07	94.07
22809-5	7963	17.49	7.25	92.77	0.43	437	0.70	530	2.5	215.74	41.45	0.07	100.02
22809-6	7964	10.72	5.68	50.90	0.43	437	0.70	475	4.0	118.37	52.99	0.10	56.58
22809-7	7965	13.73	5.70	68.08	0.39	436	0.69	496	2.8	174.56	41.51	0.08	73.78
22809-8	7966	10.82	5.24	47.52	0.56	434	0.65	439	5.2	84.86	48.43	0.10	52.76
22809-9	7967	18.23	6.62	98.85	0.45	434	0.65	542	2.5	219.67	36.31	0.06	105.47
22809-10	7968	13.78	6.21	64.31	0.70	436	0.69	467	5.1	91.87	45.07	0.09	70.52
22809-11	7969	15.00	6.59	78.86	0.49	439	0.73	526	3.3	160.94	43.93	0.08	85.45
22809-12	7970	13.68	6.28	68.31	0.50	427	0.52	499	3.7	136.62	45.91	0.08	74.59
22809-13	7971	12.77	6.39	52.02	0.52	433	0.63	407	4.1	100.04	50.04	0.11	58.41
22809-14	7972	14.20	6.63	74.90	0.41	436	0.68	527	2.9	182.68	46.69	0.08	81.53
22809-15	7973	16.08	7.93	86.55	0.38	435	0.66	538	2.4	227.76	49.32	0.08	94.48
22809-16	7974	10.67	7.04	45.56	0.46	437	0.71	427	4.3	99.04	65.98	0.13	52.60
22809-17	7975	15.31	7.15	77.63	0.36	434	0.66	507	2.4	215.64	46.70	0.08	84.78
22809-18	7976	15.33	7.09	77.61	0.32	433	0.63	506	2.1	242.53	46.25	0.08	84.70
22809-19	7977	14.26	6.56	71.48	0.38	433	0.63	501	2.7	188.11	46.00	0.08	78.04
22809-20	7978	15.02	6.76	78.49	0.44	429	0.56	523	2.9	178.39	45.01	0.08	85.25
22809-21	7979	10.88	4.16	55.89	0.26	437	0.71	514	2.4	214.96	38.24	0.07	60.05
22809-22	7980	14.48	5.08	81.52	0.30	436	0.70	563	2.1	271.73	35.08	0.06	86.60
22809-23	7981	13.54	4.80	75.37	0.37	435	0.67	557	2.7	203.70	35.45	0.06	80.17
22809-24	7982	13.67	4.10	78.52	0.20	435	0.66	574	1.5	392.60	29.99	0.05	82.62
Average		14.26	5.95	73.03	0.43	435	0.66	509	3.08	185.23	42.22	0.08	78.98

Table 3. Rock–Eval pyrolysis result for well 26745

Sample	Depth	TOC	S1	S2	S3	Tmax	Calc.	HI	OI	S2/S3	S1/TOC * 100	PI	S1+S2

WELL #26745													
Member: Lower Bakken Shale													
Sample	Depth	TOC	S1	S2	S3	Tmax	Calc.	HI	OI	S2/S3	S1/TOC * 100	PI	S1+S2
# ID	(ft)	wt%	Mg HC/ g rock	mg HC/ g rock	Mg CO2 /g rock	(°C)	% Ro	mg HC / g TOC	MgCO2 /g TOC				
26745-1	8691	16.18	4.08	92.35	0.31	431	0.61	571	1.9	297.90	25.22	0.04	96.43
26745-2	8692	22.19	5.91	125.69	0.42	436	0.69	566	1.9	299.26	26.63	0.04	131.60
26745-3	8693	18.20	5.78	102.81	0.44	430	0.58	565	2.4	233.66	31.76	0.05	108.59
26745-4	8694	20.88	6.84	119.56	0.45	431	0.60	573	2.2	265.69	32.76	0.05	126.40
26745-5	8695	11.87	4.68	60.09	0.52	433	0.64	506	4.4	115.56	39.43	0.07	64.77
26745-6	8696	13.55	5.67	74.65	0.47	432	0.62	551	3.5	158.83	41.85	0.07	80.32
26745-7	8697	15.73	5.47	86.42	0.45	435	0.67	549	2.9	192.04	34.77	0.06	91.89
26745-8	8698	15.96	5.47	86.96	0.47	434	0.66	545	2.9	185.02	34.27	0.06	92.43
26745-9	8699	18.50	6.32	103.93	0.41	434	0.65	562	2.2	253.49	34.16	0.06	110.25
26745-10	8700	20.20	5.86	116.38	0.50	427	0.53	576	2.5	232.76	29.01	0.05	122.24
26745-11	8701	17.28	5.33	96.19	0.45	434	0.66	557	2.6	213.76	30.84	0.05	101.52
26745-12	8702	15.33	5.54	82.50	0.35	431	0.61	538	2.3	235.71	36.14	0.06	88.04
26745-13	8703	18.41	6.37	105.80	0.35	433	0.63	575	1.9	302.29	34.60	0.06	112.17
26745-14	8704	20.49	7.66	107.71	0.41	431	0.60	526	2.0	262.71	37.38	0.07	115.37
26745-15	8705	14.35	5.49	77.18	0.55	429	0.57	538	3.8	140.33	38.26	0.07	82.67
26745-16	8706	11.43	5.43	62.75	0.44	435	0.67	549	3.8	142.61	47.51	0.08	68.18
26745-17	8707	13.97	5.07	79.21	0.43	433	0.64	567	3.1	184.21	36.29	0.06	84.28
26745-18	8708	12.65	5.26	71.19	0.48	434	0.65	563	3.8	148.31	41.58	0.07	76.45
26745-19	8709	12.77	4.85	71.63	0.31	434	0.64	561	2.4	231.06	37.98	0.06	76.48
26745-20	8710	10.90	4.81	58.43	0.33	435	0.68	536	3.0	177.06	44.13	0.08	63.24
26745-21	8711	9.81	5.55	50.37	0.28	437	0.70	513	2.9	179.89	56.57	0.10	55.92
26745-22	8712	15.64	5.51	91.74	0.31	433	0.63	587	2.0	295.94	35.23	0.06	97.25
26745-23	8713	15.51	6.18	83.49	0.27	432	0.61	538	1.7	309.22	39.85	0.07	89.67
26745-24	8714	15.65	5.13	91.28	0.21	432	0.62	583	1.3	434.67	32.78	0.05	96.41
Average		15.73	5.59	87.43	0.40	433	0.63	554	2.6	228.83	36.63	0.06	93.02

Table 4. Rock–Eval pyrolysis result for well 28042

Sample	Depth	TOC	S1	S2	S3	Tmax	Calc.	HI	OI	S2/S3	S1/TOC * 100	PI	S1+S2
# ID	(ft)	wt%	mg HC /g rock	mg HC/ g rock	Mg CO2 /g rock	(°C)	% Ro	Mg HC /g TOC	mgCO2/ g TOC				
28042-1	7954	15.70	6.86	80.31	0.58	431	0.59	512	3.7	138.47	43.69	0.08	87.17
28042-2	7955	18.62	6.30	103.46	0.54	431	0.60	556	2.9	191.59	33.83	0.06	109.76
28042-3	7956	23.24	6.66	135.69	0.49	430	0.59	584	2.1	276.92	28.66	0.05	142.35
28042-4	7957	20.67	6.11	118.86	0.53	431	0.60	575	2.6	224.26	29.56	0.05	124.97
28042-5	7958	11.95	4.24	59.88	0.61	432	0.62	501	5.1	98.16	35.48	0.07	64.12
28042-6	7959	13.15	4.85	71.41	0.49	432	0.62	543	3.7	145.73	36.88	0.06	76.26
28042-7	7960	19.47	6.71	105.96	0.49	429	0.56	544	2.5	216.24	34.46	0.06	112.67
28042-8	7961	17.27	5.86	91.69	0.60	431	0.59	531	3.5	152.82	33.93	0.06	97.55
28042-9	7962	17.51	5.93	96.32	0.50	431	0.60	550	2.9	192.64	33.87	0.06	102.25
28042-10	7963	17.53	7.30	93.83	0.69	432	0.62	535	3.9	135.99	41.64	0.07	101.13
28042-11	7964	18.17	7.28	97.83	0.47	431	0.60	538	2.6	208.15	40.07	0.07	105.11
28042-12	7965	20.12	8.60	109.88	0.56	430	0.58	546	2.8	196.21	42.74	0.07	118.48
28042-13	7966	17.10	6.84	94.57	0.58	433	0.63	553	3.4	163.05	40.00	0.07	101.41
28042-14	7967	18.56	6.43	94.11	0.56	431	0.59	507	3.0	168.05	34.64	0.06	100.54
28042-15	7968	13.25	5.88	71.47	0.53	432	0.62	539	4.0	134.85	44.38	0.08	77.35
28042-16	7969	11.06	5.12	54.51	0.45	432	0.61	493	4.1	121.13	46.29	0.09	59.63
28042-17	7970	13.53	5.35	71.15	0.47	432	0.62	526	3.5	151.38	39.54	0.07	76.50
28042-18	7971	16.21	6.36	93.38	0.35	432	0.62	576	2.2	266.80	39.24	0.06	99.74
28042-19	7972	17.95	7.59	95.89	0.36	429	0.57	534	2.0	266.36	42.28	0.07	103.48
28042-20	7973	18.00	7.75	87.52	0.67	425	0.49	486	3.7	130.63	43.06	0.08	95.27
28042-21	7974	10.94	5.02	55.37	0.53	432	0.62	506	4.8	104.47	45.89	0.08	60.39
28042-22	7975	9.31	6.34	46.40	0.32	434	0.65	498	3.4	145.00	68.10	0.12	52.74
28042-23	7976	9.77	4.88	51.68	0.34	431	0.60	529	3.5	152.00	49.95	0.09	56.56
28042-24	7977	15.25	5.18	85.37	0.32	433	0.63	560	2.1	266.78	33.97	0.06	90.55
28042-25	7978	15.38	4.69	91.49	0.37	433	0.63	595	2.4	247.27	30.49	0.05	96.18
28042-26	7979	5.35	2.49	21.44	0.19	436	0.69	401	3.6	112.84	46.54	0.10	23.93
28042-27	7980	7.43	5.60	31.90	0.39	434	0.65	429	5.2	81.79	75.37	0.15	37.50
Average		15.28	6.01	81.90	0.48	432	0.61	528	3.3	173.69	41.28	0.07	87.91

Table 5. Rock–Eval pyrolysis result for well 23828

|														
WELL #23828														
Member: Lower Bakken Shale														
Sample	Depth	TOC	S1	S2	S3	Tmax	Calc.	HI	OI	S2/S3	S1/TOC * 100	PI	S1+S2
# ID	(ft)	wt%	Mg HC /g rock	mg HC/ g rock	Mg CO2 /g rock	(°C)	% Ro	mg HC /g TOC	MgCO2 / g TOC				
23828-1	7934	18.07	6.53	98.75	0.53	429	0.57	546	2.9	186.32	36.14	0.06	105.28
23828-2	7935	11.28	5.42	59.54	0.53	432	0.62	528	4.7	112.34	48.05	0.08	64.96
23828-3	7936	7.73	3.79	36.89	0.43	431	0.60	477	5.6	85.79	49.03	0.09	40.68
23828-4	7937	13.03	6.09	68.11	0.56	431	0.60	523	4.3	121.63	46.74	0.08	74.20
23828-5	7938	13.00	6.12	68.41	0.55	430	0.58	526	4.2	124.38	47.08	0.08	74.53
23828-6	7939	18.83	7.51	100.65	0.57	430	0.58	535	3.0	176.58	39.88	0.07	108.16
23828-7	7940	14.35	5.49	77.18	0.55	429	0.57	538	3.8	140.33	38.26	0.07	82.67
23828-8	7941	10.28	5.26	52.04	0.38	432	0.62	506	3.7	136.95	51.17	0.09	57.30
23828-9	7942	12.73	5.54	68.50	0.39	429	0.55	538	3.1	175.64	43.52	0.07	74.04
23828-10	7943	15.97	6.64	87.31	0.39	429	0.55	547	2.4	223.87	41.58	0.07	93.95
23828-11	7944	16.92	6.77	91.29	0.41	428	0.54	540	2.4	222.66	40.01	0.07	98.06
23828-12	7945	18.17	6.76	99.89	0.46	429	0.56	550	2.5	217.15	37.20	0.06	106.65
23828-13	7946	13.62	4.55	75.14	0.39	431	0.59	552	2.9	192.67	33.41	0.06	79.69
23828-14	7947	6.90	2.28	30.62	0.28	435	0.67	444	4.1	109.36	33.04	0.07	32.90
Average		13.63	5.63	72.45	0.46	430	0.58	525	3.5	158.98	41.79	0.07	78.08
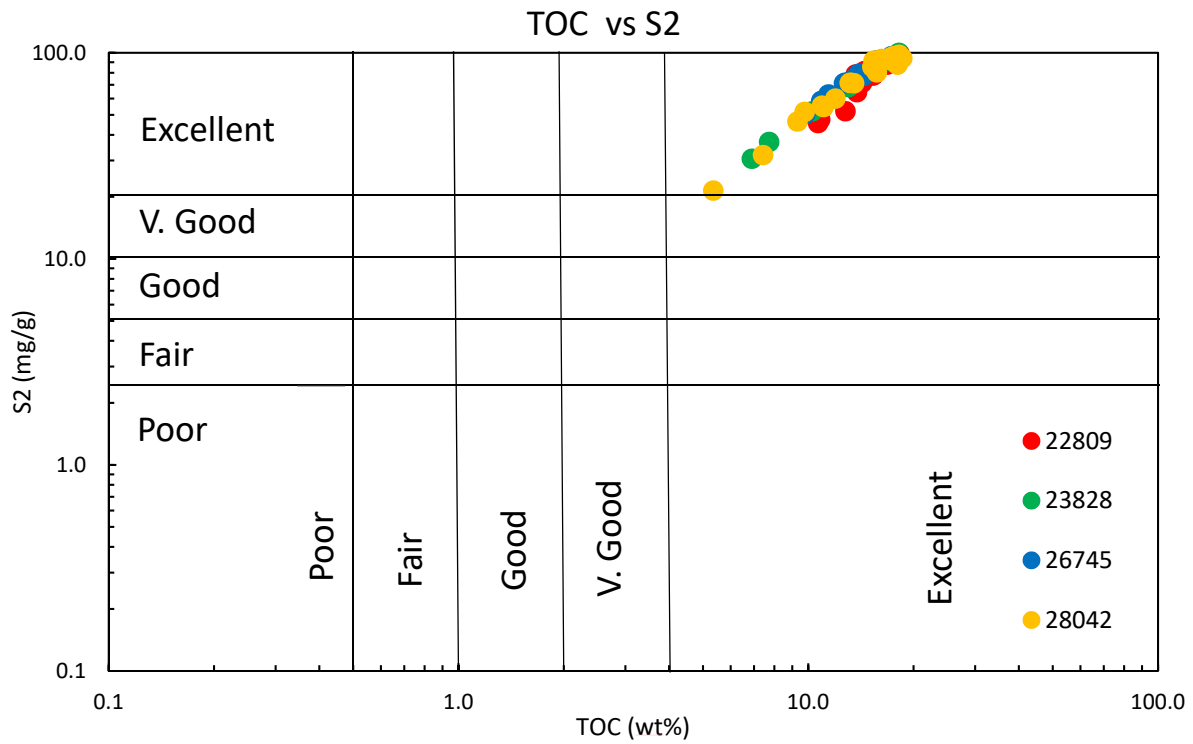
Figure 23. Quantity and quality of organic matter in the studied wells from TOC and S2 analysis
45

Generating potentials

The results of the pyrolysis can be utilized to evaluate the potential of the source rock to generate hydrocarbon. Hunt 1996 evaluated and classified the generating potential (GP) of a source rock with the summation of S1 and S2 values. Accordingly, he classified GP < 2 for a poor source rock, 2 to 5, for fair, 5-10 for good and > 10 are considered to have a very good GP. For the purpose of this work, I modified 10-20 as very good and > 20 as excellent. All the data points in the studied wells have excellent generating potential based on the plot of TOC vs S1+S2 (Figure 25).

Thermal maturity of organic matter

Thermal maturity of organic matter during burial influences hydrocarbon. The type of organic matter and intensity of thermal alteration has the most control on hydrocarbon distribution in a source rock. Thermal maturity is determined by various maturity indices, this study utilizes the Tmax values of the S2 peak from pyrolysis to compare maturity across wells. Peters 1986 indicated source rock begin oil generation at Tmax 435-465°C and gas at 470°C. A plot of Tmax vs HI (Figure 26) compares source rock maturity and kerogen types in the studied wells. The results showed that all the wells have varying degrees of maturity, with well 22809 having the most data points across the 435°C maturity line. Wells 28042 and 23828 have almost all of their data points in the immature zone, while well 26745 has more data point than wells 28042 and 23838 across the maturity line. Also Wells 22809, 26745, 28042 and 23828 have a Tmax average of 435°C, 433°C, 432°C and 430°C respectively. From these results, well 22809 is the most matured while 23838 is the least matured. Well 26745 is more mature that well 28042.
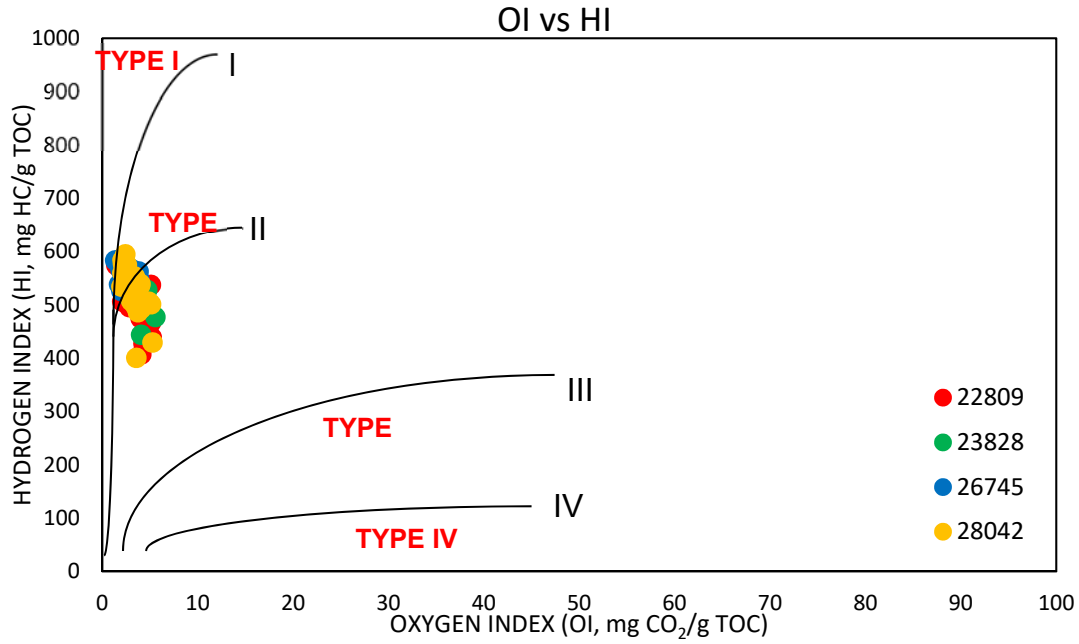
Figure 24. Organic matter types of the Lower Bakken source rock as indicated from OI and HI.
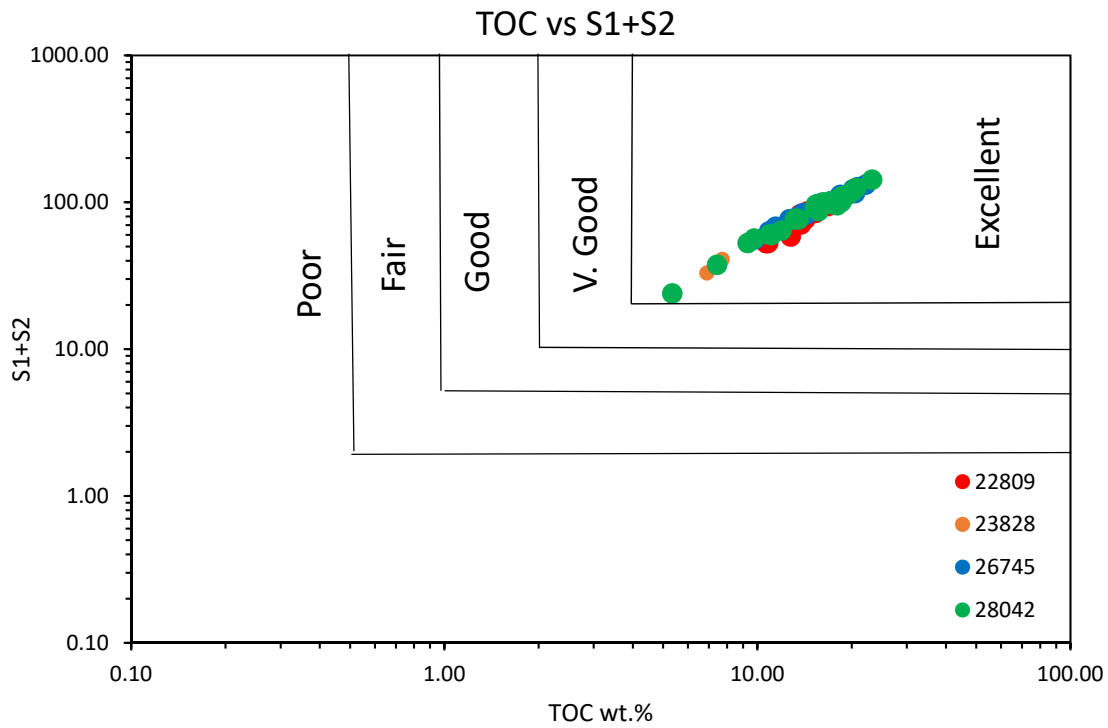

Figure 25. Generative potentials of the Lower Bakken source rock from TOC vs S1+S2.
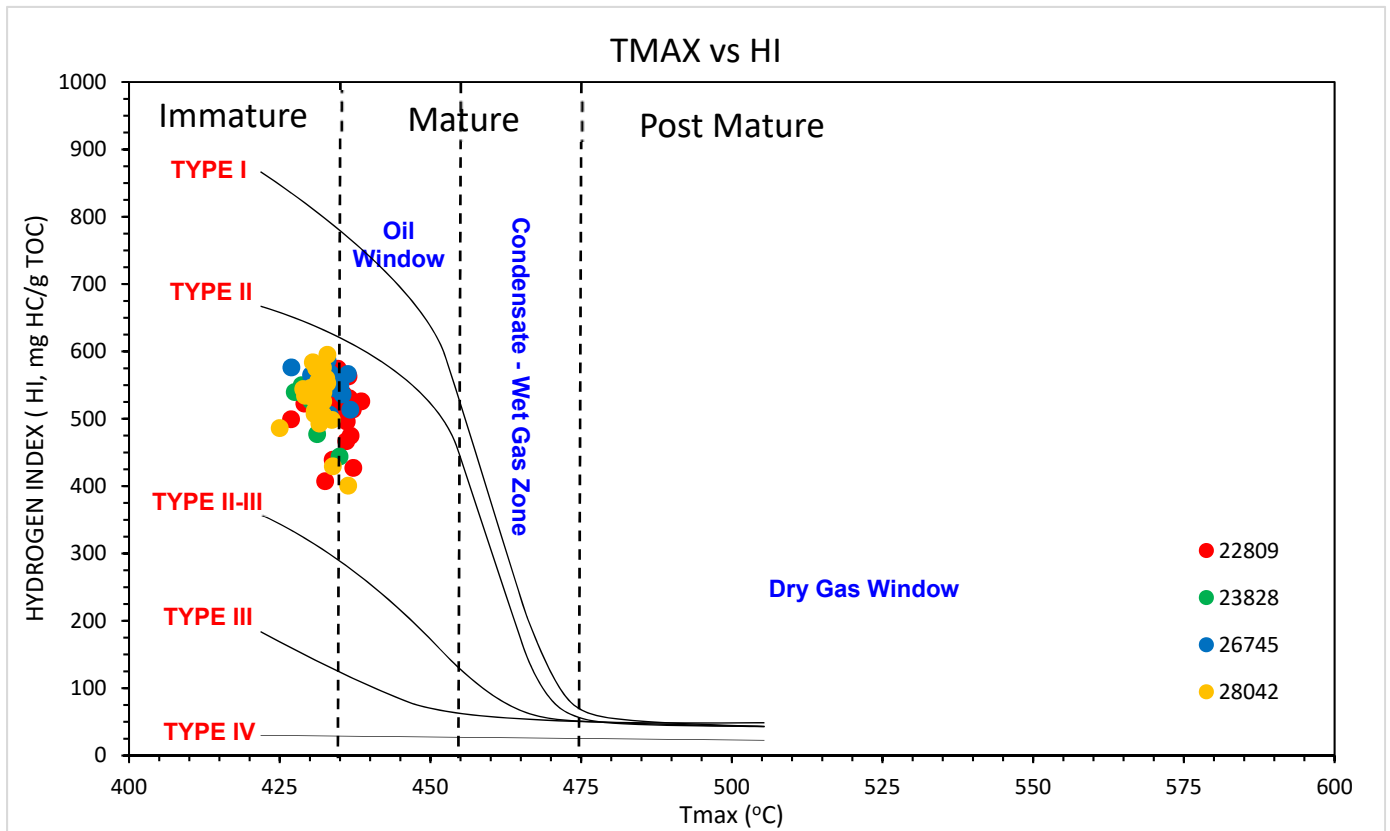
Figure 26. Thermal maturation and types of organic matter from Tmax and HI.

Porosity Results

Helium Porosimeter.

The results of the porosity measurements from helium porosimeter are displayed in Tables 6, 7, 8, 9 and 10 for wells 22809, 26745, 28042 and 23828 respectively. Analysis was ran five (5) time on each samples for quality check and quality control. The output of the analysis are grain volume, pore volume, grain density, bulk density and porosity. The Lower Bakken shale has the lowest pore volumes, grain and bulk densities, this is due to the low density of organic making up the shale composition. Their grain densities range from 2.16 – 2.26 g/ml, while bulk volume range from 2.08 – 2.20 g/ml and pore volumes from 0.12 – 0.27 ml. The massive dolostones have the highest grain and bulk densities, which is a result of the high density of dolomite minerals that make up their composition. They range from 2.80 – 2.82 g/cm^3 and 2.68 – 2.75 g/cm^3 for grain density and bulk density respectively. The massive mudstones and mottled mudstones have relatively high porosity values, ranging from 7.83 to 11.71 % for massive mudstone and 7.12 to 9.41% for mottled mudstone. The Lower Bakken shale and massive dolostone porosity values are relatively low, ranging from 2.88 to 4.01 for the shale and 2.13 to 4.21 % for the massive dolostone. The facies with more mudstones in their composition have relatively higher porosity while shales and dolostone lithofacies have relatively low porosities (Figure 27).

Table 6. Helium porosimetry results for well 22809

			WELL 22809					
Facies	S/N	Mass	Bulk volume	Grain volume	Pore volume	Grain density	Bulk density	Φ
		g	ml	ml	ml	g/ml	g/ml	%
Laminated	1	43.44	16.93	16.118	0.82	2.70	2.57	4.82
Shale	2	16.84	8.04	7.771	0.27	2.17	2.10	3.31
Massive Dolostone	3	66.77	24.88	23.830	1.05	2.80	2.68	4.21
Mottled Dolostone	4	36.15	13.95	13.167	0.78	2.75	2.59	5.62
Mudstone conglomerates	5	27.01	10.99	10.109	0.88	2.67	2.46	7.99
Brecciated mudstone	6	42.44	17.20	15.820	1.38	2.68	2.47	8.02
Mottled mudstone	7	24.07	9.81	9.001	0.81	2.67	2.45	8.25
Massive Mudstone	8	40.03	16.99	15.000	1.99	2.67	2.36	11.71

Table 7. Helium porosimetry results for well 26745

			WELL 26745					
Facies	S/N	Mass	Bulk volume	Grain volume	Pore volume	Grain density	Bulk density	Φ
		g	ml	ml	ml	g/ml	g/ml	%
Laminated	1	47.05	18.20	17.421	0.78	2.70	2.59	4.26
Shale	2	15.90	7.23	7.023	0.21	2.26	2.20	2.88
Massive Dolostone	3	25.63	9.50	9.132	0.37	2.81	2.70	3.91
Mottled Dolostone	4	38.55	15.13	14.060	1.07	2.74	2.55	7.06
Mudstone conglomerates	5	30.89	12.65	11.520	1.13	2.68	2.44	8.92
Massive Mudstone	6	15.54	6.43	5.814	0.62	2.67	2.42	9.63
Mottled mudstone	7	17.50	7.22	6.653	0.56	2.63	2.42	7.81
Brecciated mudstone	8	22.66	9.46	8.590	0.87	2.64	2.40	9.21

Table 8. Helium porosimetry results for well 28042

	WELL 28042							
Facies	S/N	Mass	Bulk volume	Grain volume	Pore volume	Grain density	Bulk density	Φ
		g	ml	ml	ml	g/ml	g/ml	%
Laminated	1	36.92	14.66	13.749	0.91	2.69	2.52	6.21
Shale	2	10.32	4.96	4.760	0.20	2.17	2.08	4.01
Massive Dolostone	3	78.99	28.86	28.246	0.61	2.80	2.74	2.13
Mottled Dolostone	4	56.51	22.14	20.726	1.41	2.73	2.55	6.37
Massive Mudstone	5	21.69	8.88	8.181	0.70	2.65	2.44	7.83
Mottled mudstone	6	80.00	32.31	30.010	2.30	2.67	2.48	7.12
Mudstone conglomerates	7	37.01	14.87	13.817	1.05	2.68	2.49	7.08
Brecciated mudstone	8	41.70	16.72	15.735	0.99	2.65	2.49	5.91

Table 9. Helium porosimetry results for well 23828

|	WELL 23828							
Facies	S/N	Mass	Bulk volume	Grain volume	Pore volume	Grain density	Bulk density	Φ
		g	ml	ml	ml	g/ml	g/ml	%
Laminated	1	21.86	8.49	8.122	0.37	2.69	2.57	4.33
Shale	2	8.33	3.97	3.853	0.12	2.16	2.10	3.01
Massive Dolostone	3	49.63	18.04	17.622	0.42	2.82	2.75	2.32
Mottled Dolostone	4	31.90	12.72	11.759	0.96	2.71	2.51	7.56
Massive Mudstone	5	32.44	13.45	12.200	1.25	2.66	2.41	9.26
Mottled mudstone	6	41.51	17.32	15.690	1.63	2.65	2.40	9.41
Mudstone conglomerates	7	51.76	20.86	19.420	1.44	2.67	2.48	6.92
Brecciated mudstone	8	60.22	23.77	22.512	1.26	2.68	2.53	5.31
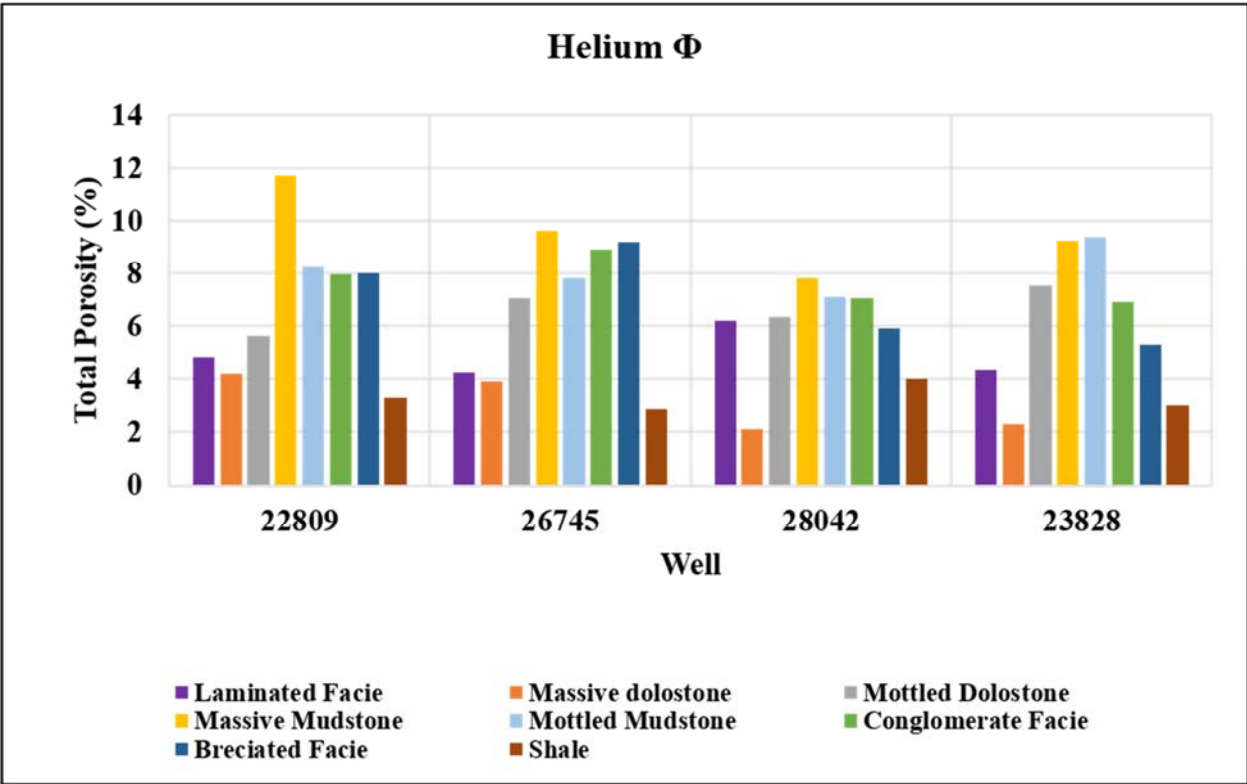
Figure 27. Helium porosity of all lithofacies in the studied wells.

NMR T2 Relaxation time

The results of the NMR transverse relaxation time analysis for all the facies are displayed in Figures 28, 29, 30 and 31 for well 22809, 26745, 28042 and 23828. The results are plots of incremental porosity in percentage versus transverse time in milliseconds. The peak of the curves correspond to the transverse relaxation time (T2) with the highest porosity value. The peak occurs at varying time on the T2 time axis depending on the pore spaces distribution within each facies. The Lower Bakken Shale and massive dolostone both have relatively low T2 peaks and NMR porosity in all wells. The massive mudstone and mottled mudstone have relatively higher T2 peaks and NMR porosity in all wells.

The T2 time distribution for each lithofacies are displayed in Figures 32-39. The Lower Bakken Shales have uniform NMR signature with the T2 peak skewing to the right (Figure 32). All the signatures are fairly superimposed which suggests a uniform lithology composition. The NMR porosity range from 2.96 – 4.25%. Laminated lithofacies have uniform NMR T2 signatures with bimodal T2 peaks (Figure 33). The bimodal peaks are attributed to the two lithologies contained in the facies, each peak corresponding to the individual lithology. Porosity within this lithofacies range from 4.71 – 6.44%. Massive dolostones have non-uniform bimordial distribution with varying T2 peaks skewing to the left (Figure 34). The difference in the uniformity is thought to be associated with the lateral variation in dolomitization. NMR porosity in this lithofacie are relatively low and range from 2.47 – 4.69%. Mottled dolostones have non-uniform NMR T2 signatures with varying T2 peaks (Figure 35). The difference in the T2 signatures are suggested to be attributed to lateral variation in dolomitization and varying proportion of mudstones present in the lithofacies. Porosity values range from 5.81 – 8.65 %.

Massive mudstones have uniform and relatively superimposed NMR T2 signatures that are almost symmetrical (Figure 36). The T2 peaks in all wells occur around the same relaxation time but varies with incremental porosity. This lithofacies have relatively high porosities that range from 8.12

– 12.08%. Mottled mudstones have uniform and superimposed signatures (Figure 37). The T2 peaks occur around the same time but also vary with incremental porosity. They have a relatively high NMR porosity ranging from 7.95 – 9.56%. Mudstone conglomerates have uniform T2 signatures that are relatively superimposed (Figure 38). The T2 peaks occur around the same time but with varying incremental porosity. They have relatively high NMR porosity that range from 8.05 – 9.39%. Brecciated mudstone lithofacies have irregular T2 signatures and varying T2 peaks in all the wells (Figure 39). This is suggested to be a result of varying proportion of dolostone contained in them. Porosity values in this lithofacie range from 5.87 to 9.58%

The massive mudstone lithofacies have the highest NMR porosities in all wells, followed by mottled mudstone lithofacie with the second highest porosity (Figure 40). In addition, the Lower Bakken shale and massive dolostone lithofacies have the least porosities. Other lithofacies have intermediate porosities within these extremes. The R-squared coefficient is 0.985, which is very close to 1. This shows a close relationship between the two methods of porosity estimation (Figure 41).
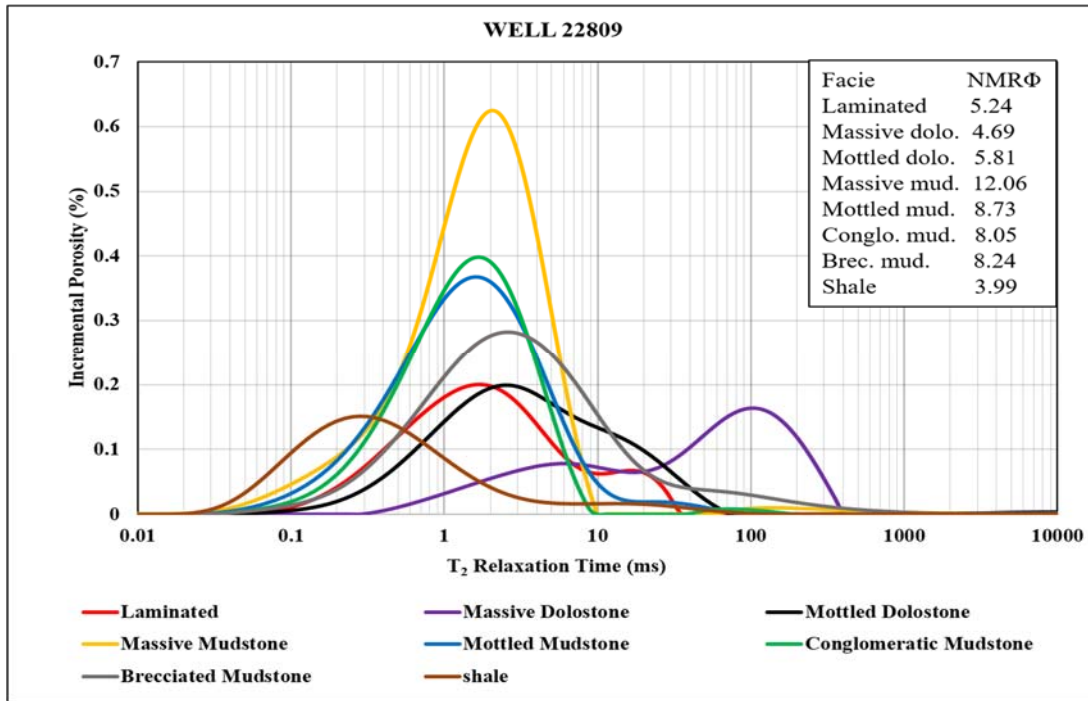
Figure 28. T2 Relaxation time and incremental porosity plot for well 22809
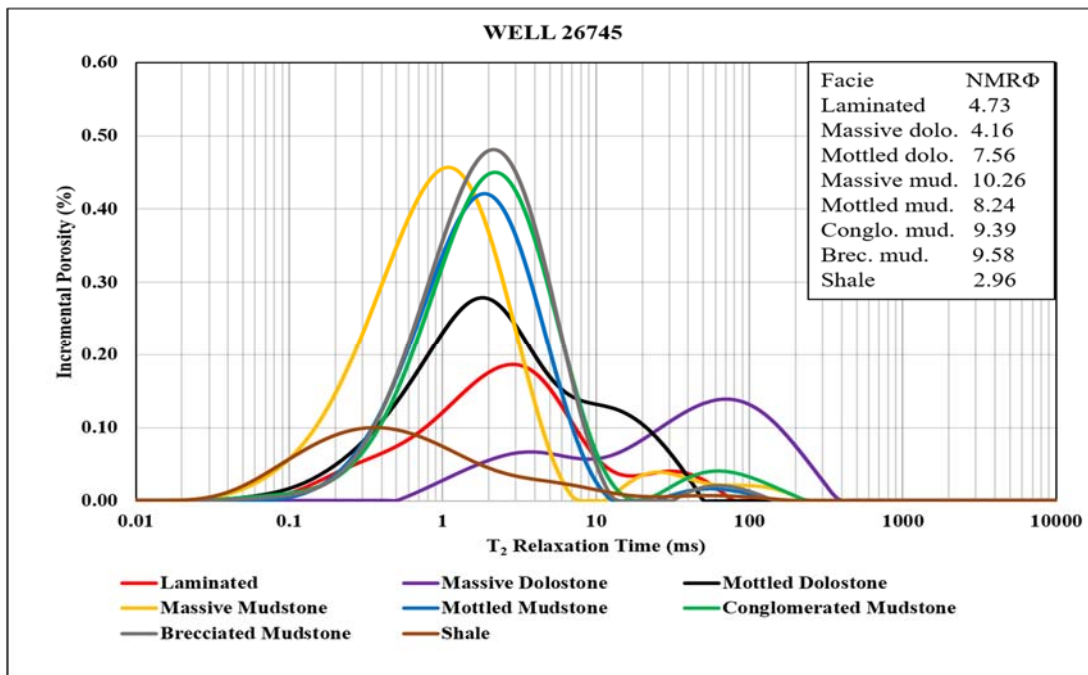
Figure 29. T2 Relaxation time and incremental porosity plot for well 26745
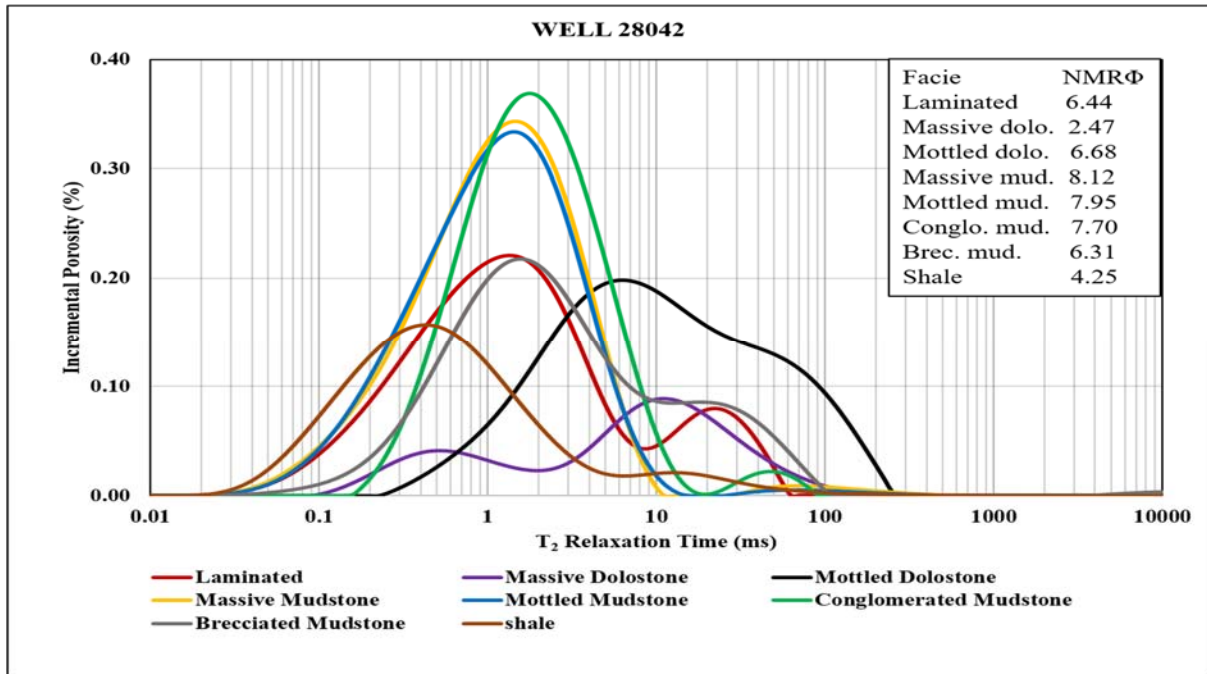
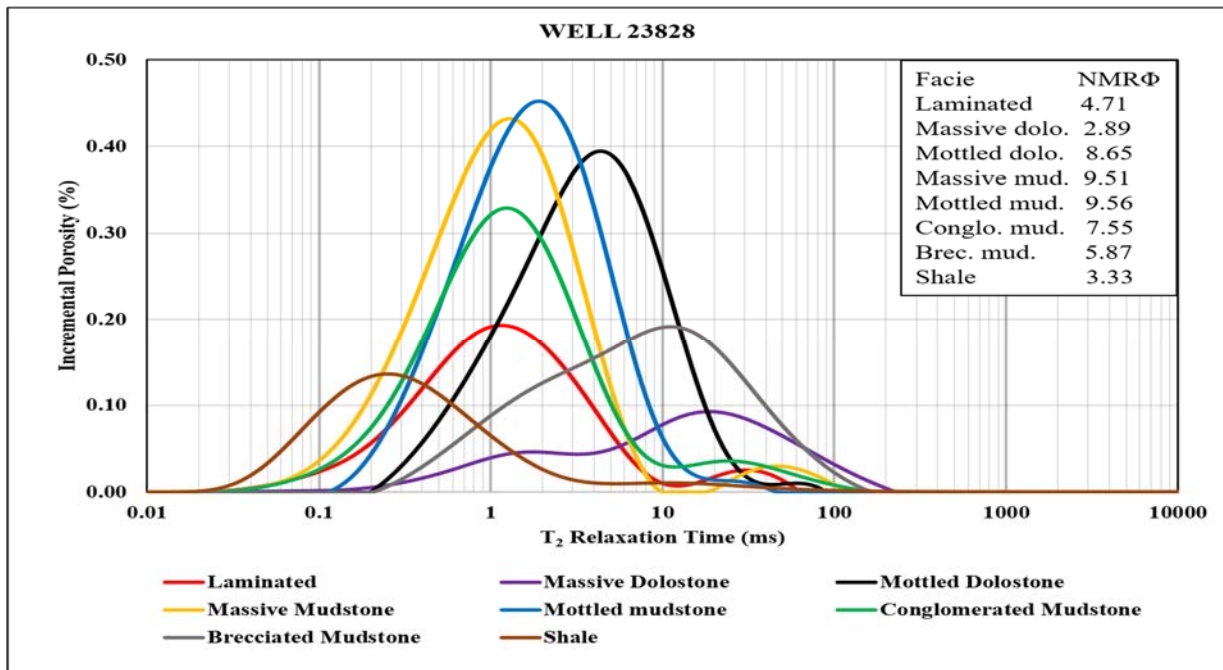Figure 30. T2 Relaxation time and incremental porosity plot for well 28042

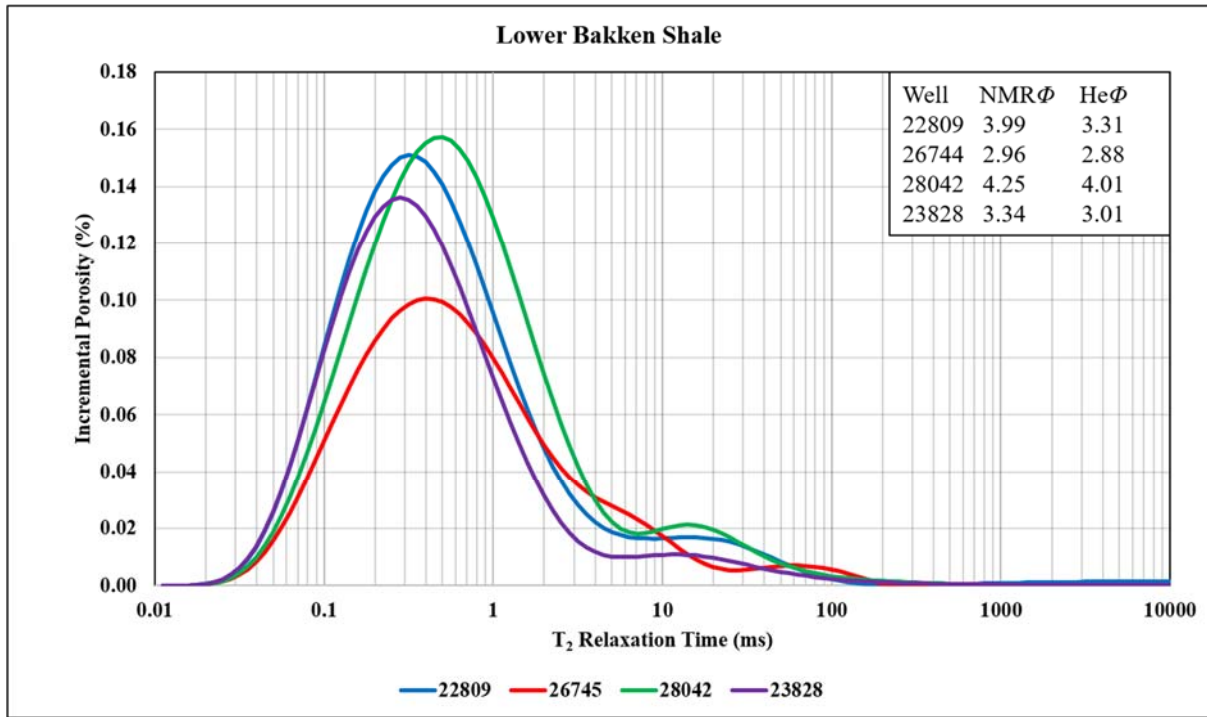Figure 31. T2 Relaxation time and incremental porosity plot for well 23828

Figure 32. T2 Relaxation time and incremental porosity plot for the Lower Bakken Shale
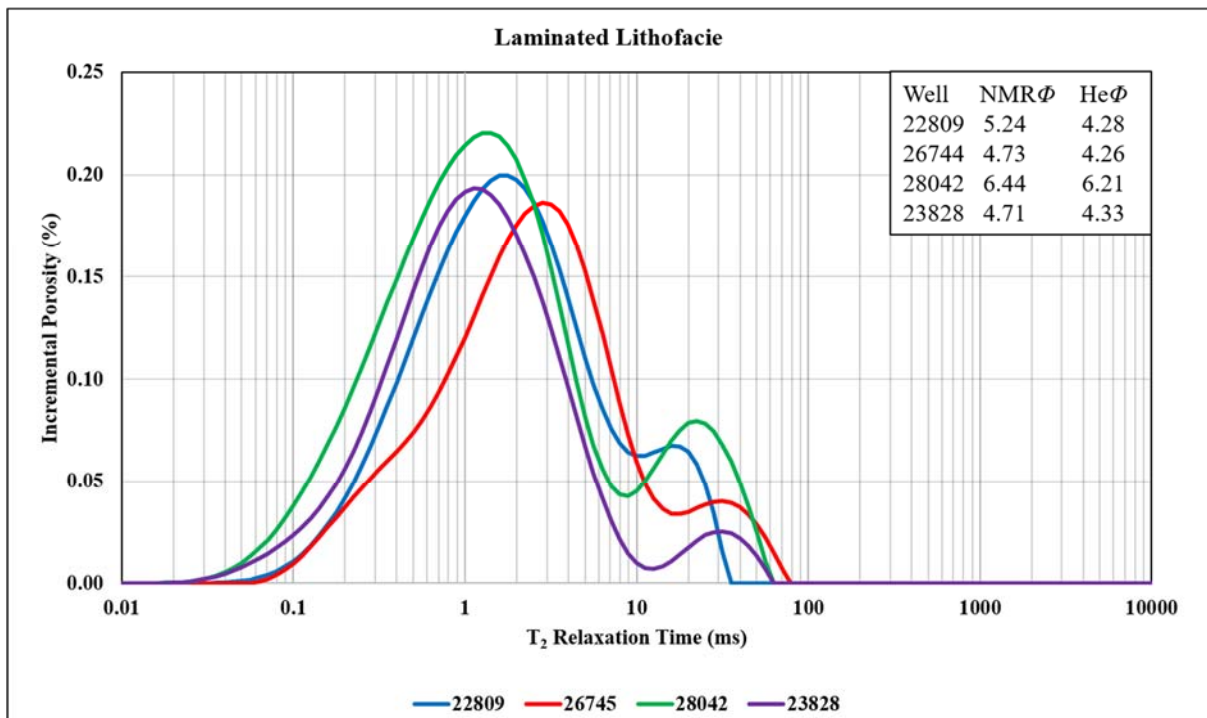

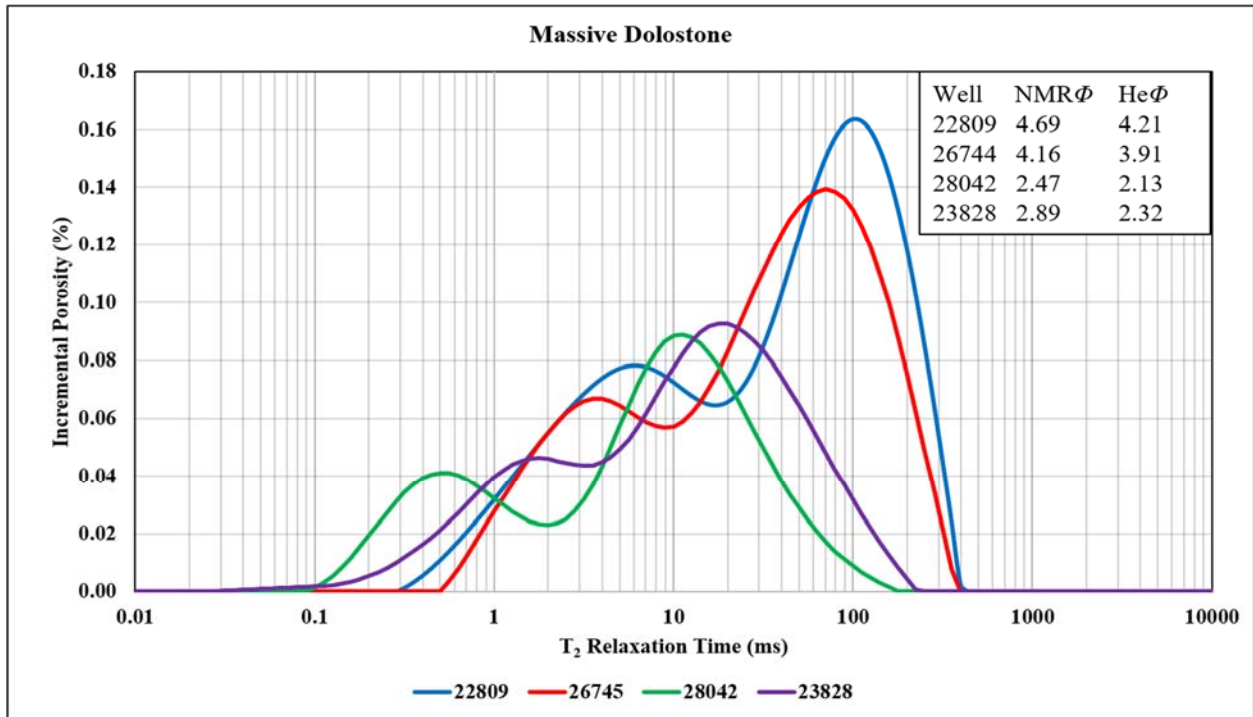Figure 33. T2 Relaxation time and incremental porosity plot for the laminated lithofacies

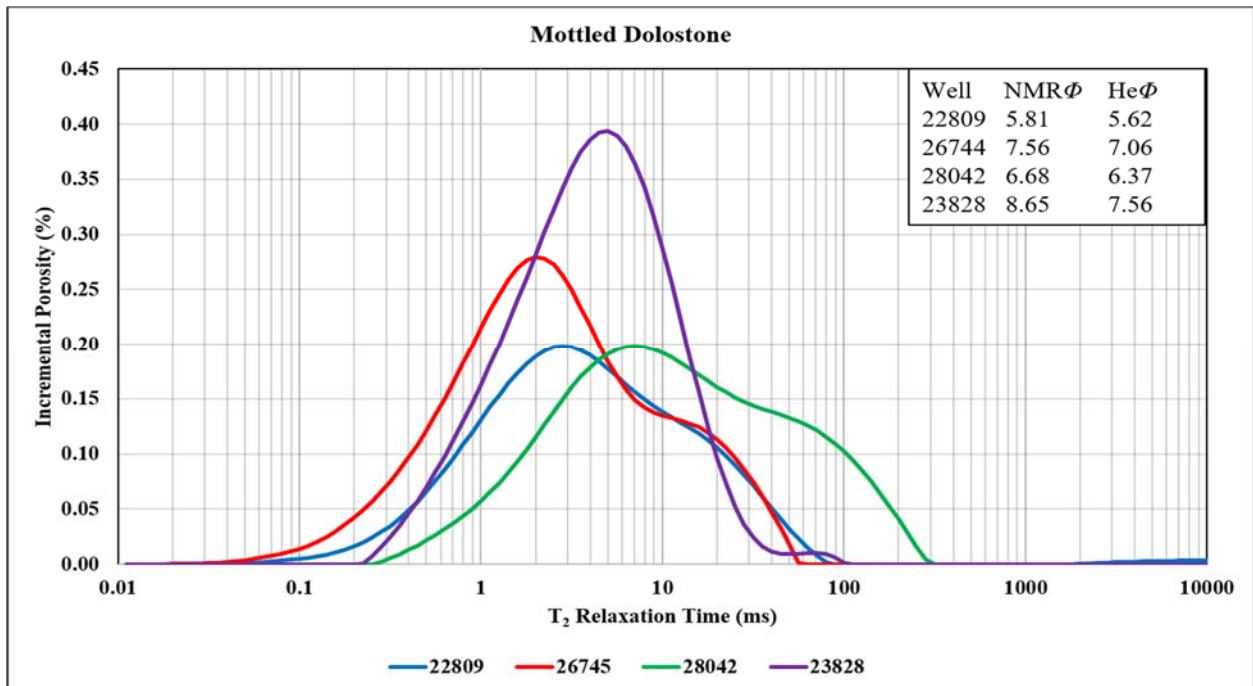Figure 34. T2 Relaxation time and incremental porosity plot for the massive dolostone lithofacie

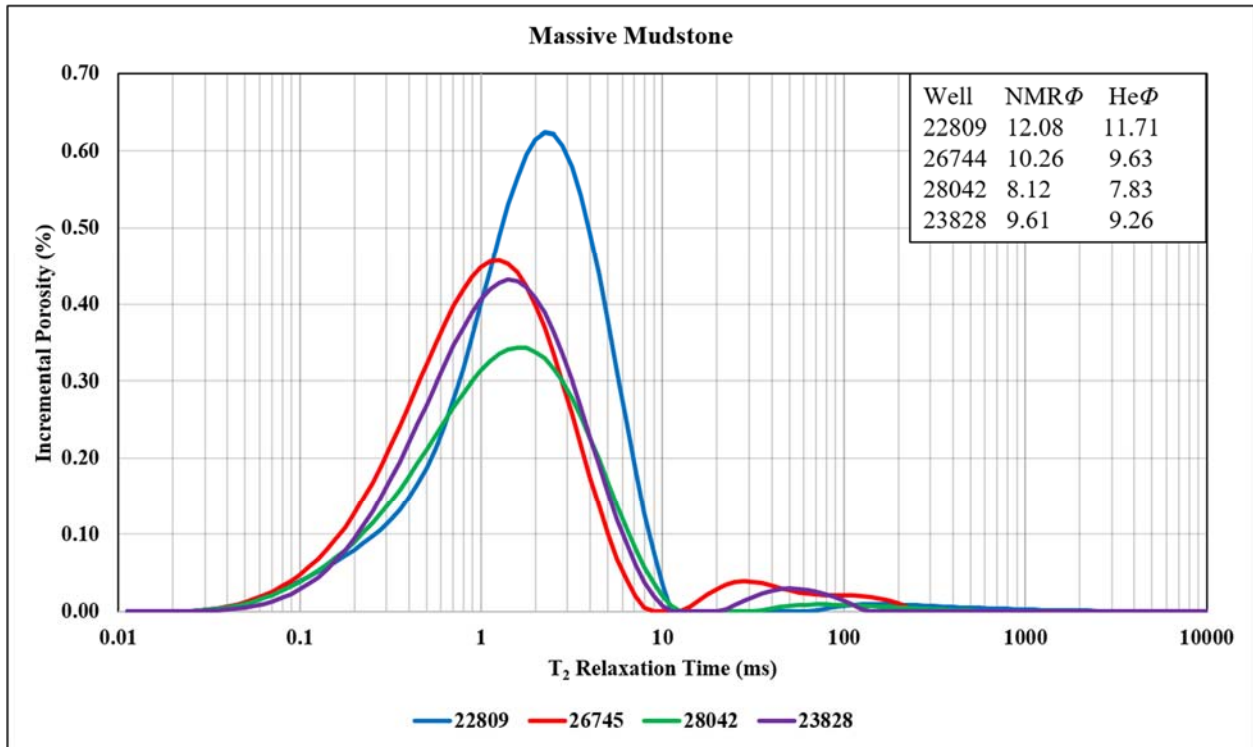Figure 35. T2 Relaxation time and incremental porosity plot for mottled dolostone lithofacie

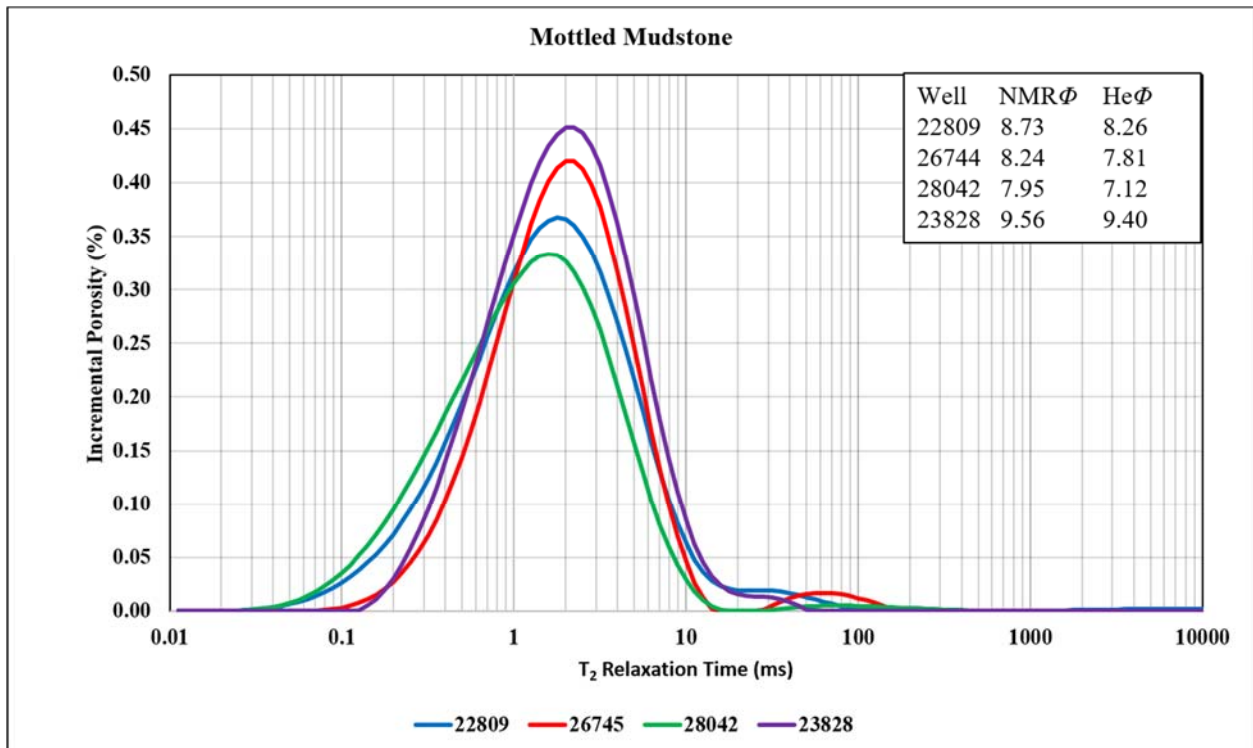Figure 36. T2 Relaxation time and incremental porosity plot for the massive mudstone lithofacie

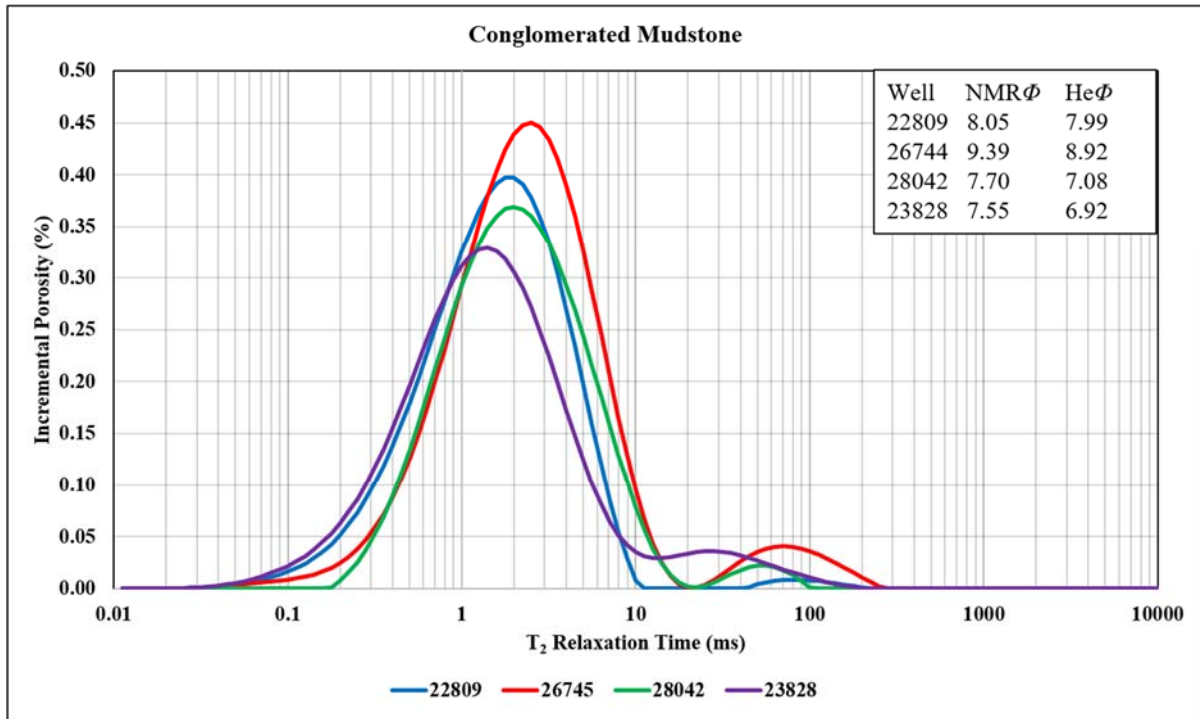Figure 37. T2 Relaxation time and incremental porosity plot for the mottled mudstone litofacie

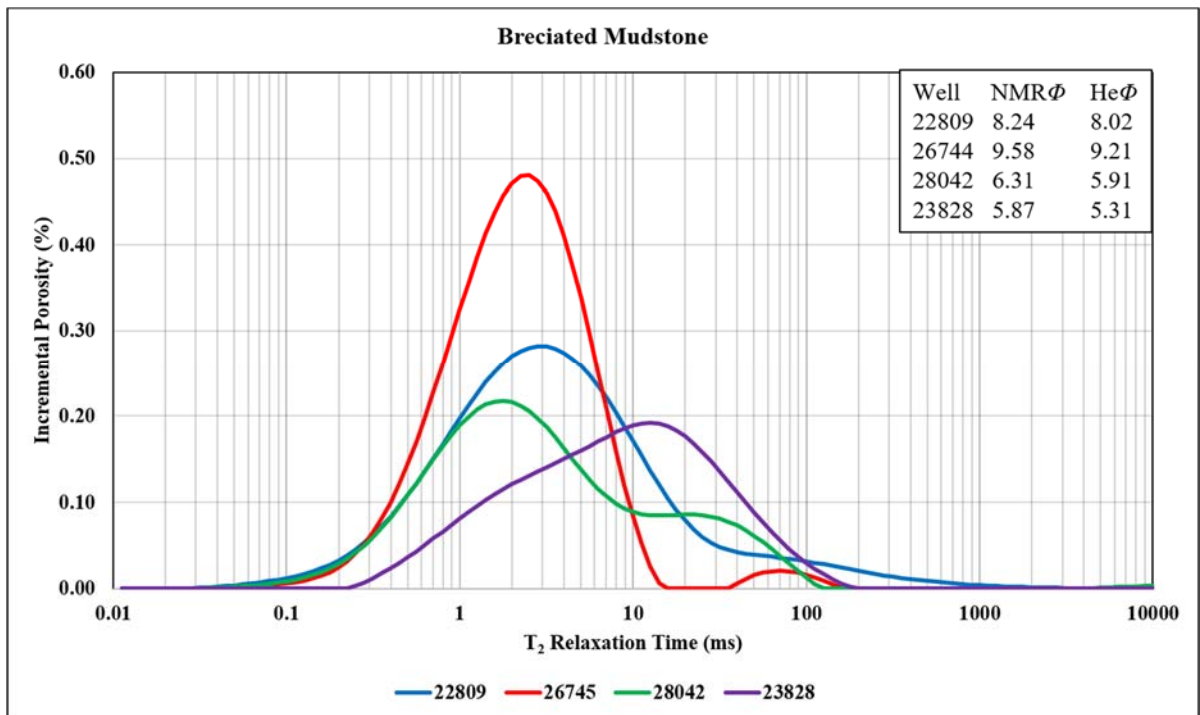Figure 38. T2 Relaxation time and incremental porosity plot for the conglomerated mudstone lithofacie

Figure 39. T2 Relaxation time and incremental porosity plot for the brecciated mudstone lithofacie
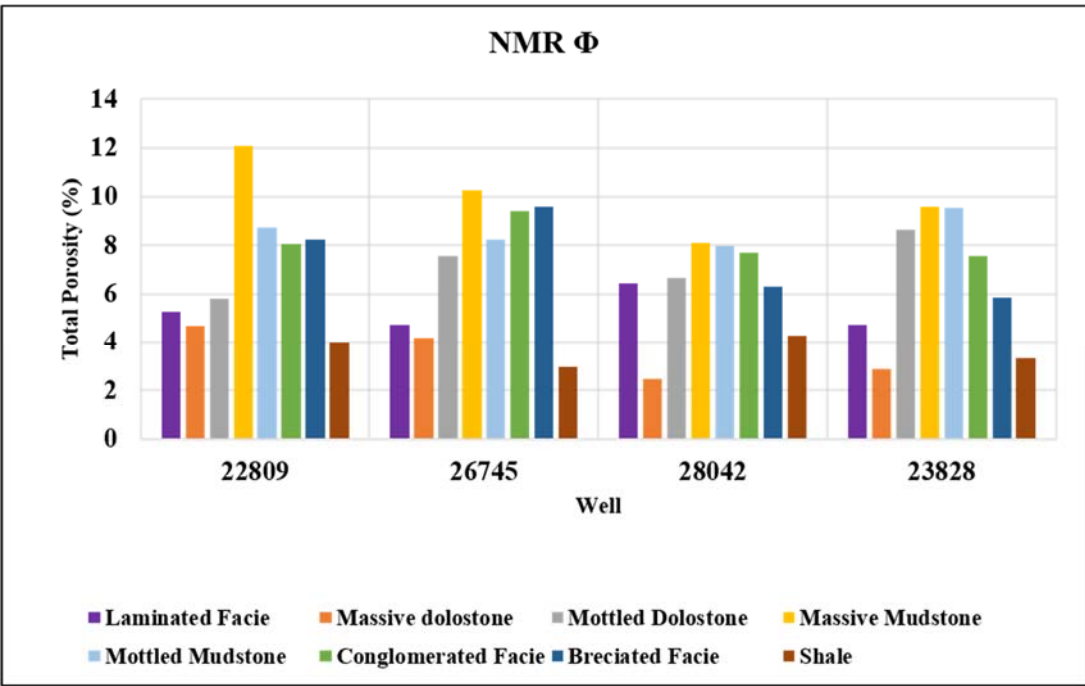
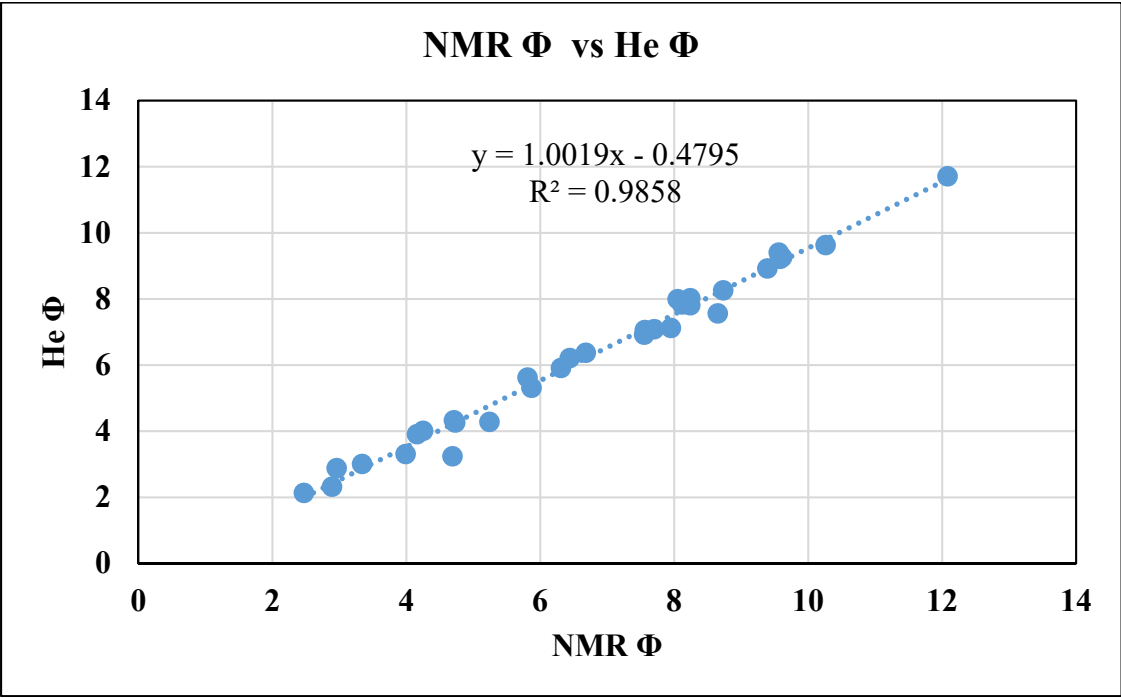Figure 40. NMR porosity for all lithofacies in the study wells

Figure 41. Plot of NMR porosity vs He porosity

Pore Sizes Distribution

The various fluid types and their distributions within the pore space can be reflected in the overall NMR response (Figure 42). NMR can differentiate clay-bound from capillary-bound and movable water with the T2 cutoff each phase is located in a different portion of the pore space (Basan 2010).

T2 cutoffs for the different pore sizes and fluids are dependent on the rock type and pore geometry. A variable cutoff will represent the variation in the pore size properties. The variation in T2 cutoffs is expected as a result of the change in the porous media pores sizes. Cutoffs values are determined in the laboratory by measuring the NMR T2 relaxation times under saturated and desaturated conditions. The cutoff values of Allen et al 2001 were calibrated with sandstone reservoirs and were found to be different for tight lithologies and presence of fractures (Romero and Mantoya 2001). Green and Vaselinovic 2010 argued that applying the traditional T2 cut of 33ms for unconventional reservoirs would result in overestimation of bound water due to higher capillary pressure and larger transition region, thereby lowering the estimated recoverable reserves. They propose a cutoff of 1ms and 10 ms for the bound water and free fluids respectively in low permeability reservoirs.

Allen et. al (2001) characterized the reservoir pore system of a studied core by subdividing it into three components defined by the pore throat diameter as measured by mercury injection. He classified them into micropores, mesopores and macropores. Micropores are the smallest pores (throat < 0.5 micron, contains mostly irreducible water), mesopores are medium size (throat between 0.5 and 5 micros, contains formation water and hydrocarbons), and macropores which are the largest pores (throat > 5 microns, contains mainly movable fluids). He further tied the portioned pores to the NMR T2 cutoff with the small and large cutoff corresponding to the micropores and

macropores respectively. Al-Marzouqi et al (2010) created a diagrammatic representation of (Allen et. al 2000) partitioned porosities with reservoir fluids, pore diameter and NMR T2 cutoff (Figure 43).

The plots of NMR T2 results for individual lithofacies are displayed in Figures 43 – 50. It can be seen that the Lower Bakken shale is made of up > 70% micropores which are filled with clay bound water in all wells (Figure 44). This gives an explanation to the issue of Bakken Shale being a poor hydrocarbon reservoir, even after fracking. The mudstone lithofacies (massive mudstone, mottled mudstone, conglomerated mudstone and brecciated mudstones) are mainly composed of >50% mesopores, with micropores and extremely low macropores (Figure 48-51). The brecciated mudstone contains > 20% macropores in wells that have more dolostone breccia in them. The massive dolostone (Figure 46) and mottled dolostones (Figure 47) have higher proportions of macropores, with less mesopores and macropores. The laminated lithofacie have micropores and mesopores for the mudstone lithology and macropores for the dolostone lithology (Figure 45). Figure 52 shows the pore sizes distribution within lithofacies across study wells.
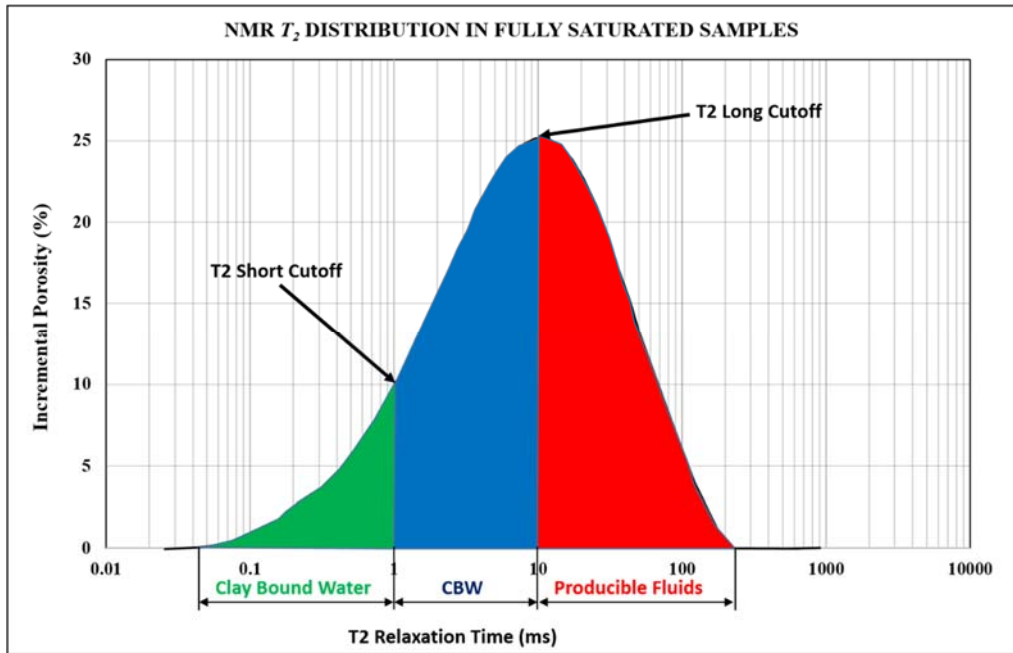
Figure 42. Model representing T2 relaxation and fluid distribution across the pore space modified after Basan (2010)
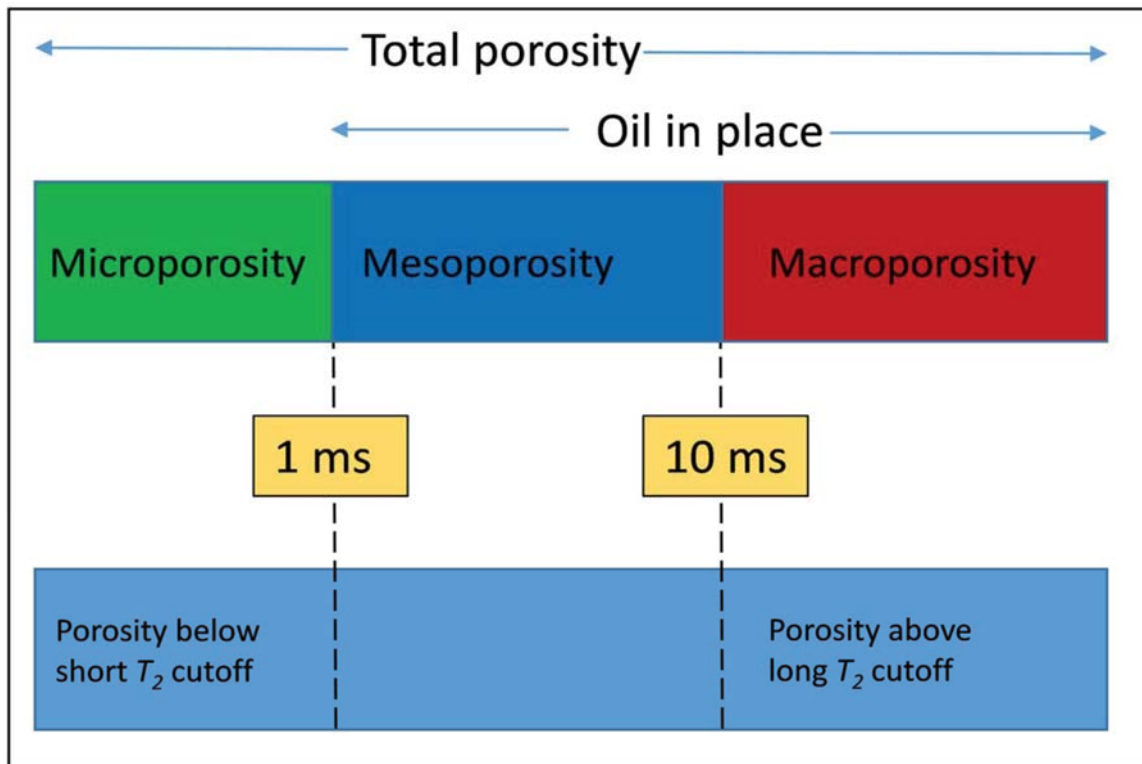
Figure 43. NMR porosity portioning with diameter, cutoff and reservoir fluids (Al-Marzouqi et. al. 2010)
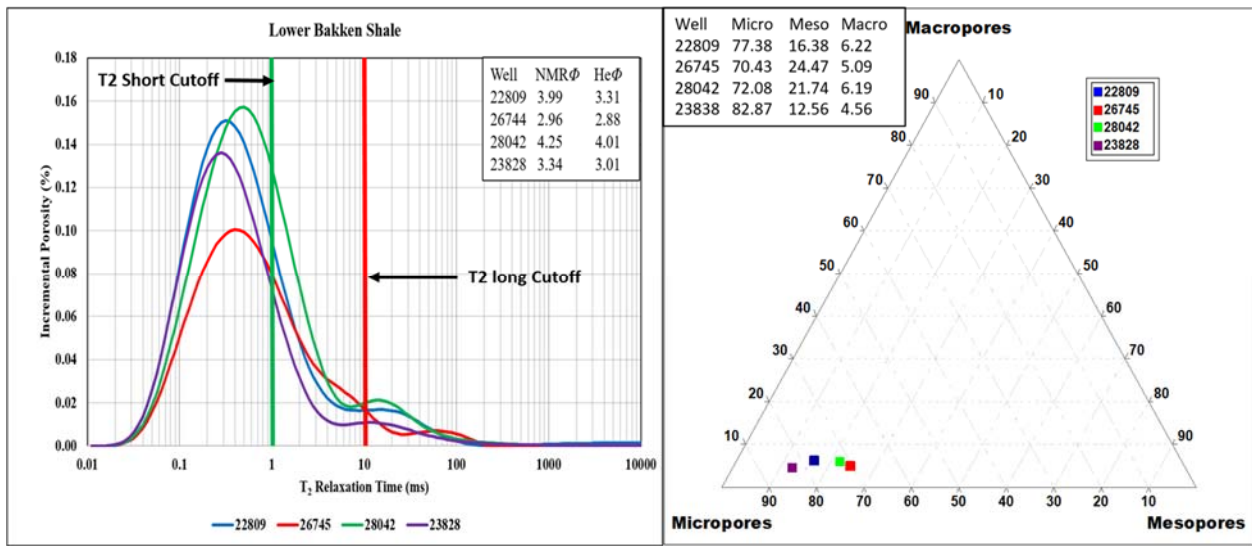
Figure 44. NMR Porosity distribution and percentage of pore types the Lower Bakken Shales

Figure 45. NMR Porosity distribution and percentage of pore types in the laminated lithofacie

Figure 46. NMR Porosity distribution and percentage of pore types in the massive dolostone lithofacie

Figure 47. NMR Porosity distribution and percentage of pore types in the mottled dolostone lithofacie

Figure 48. NMR Porosity distribution and percentage of pore types in the massive mudstone lithofacie
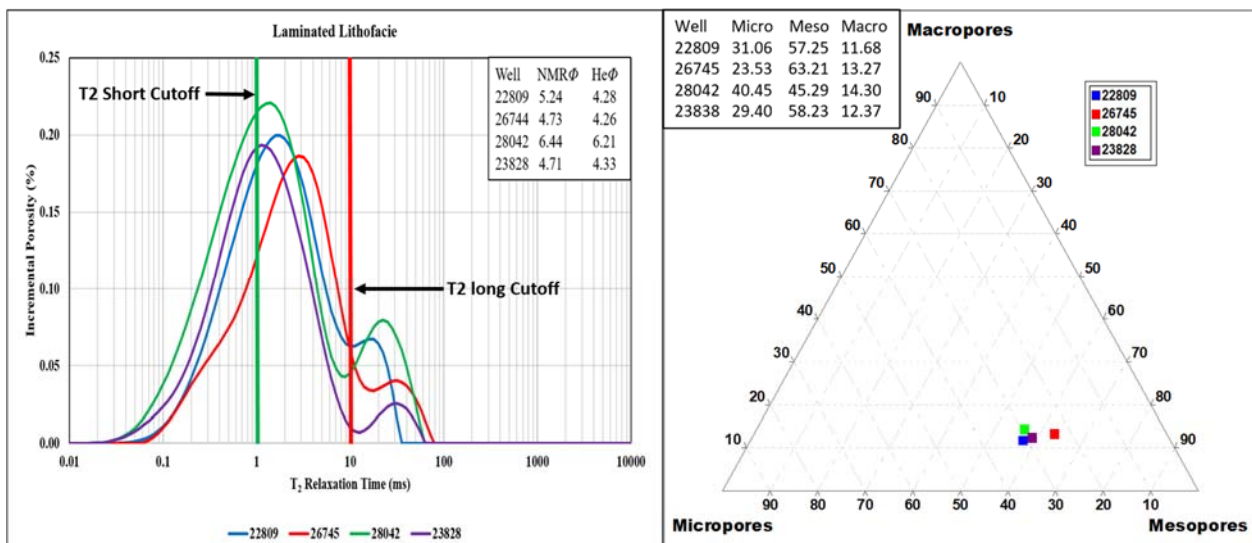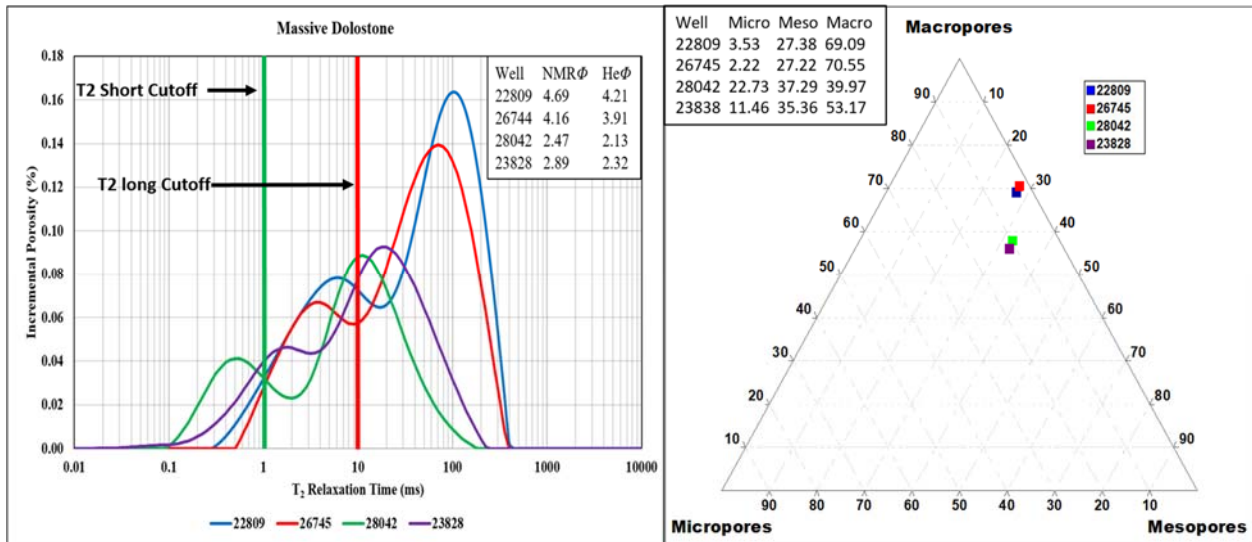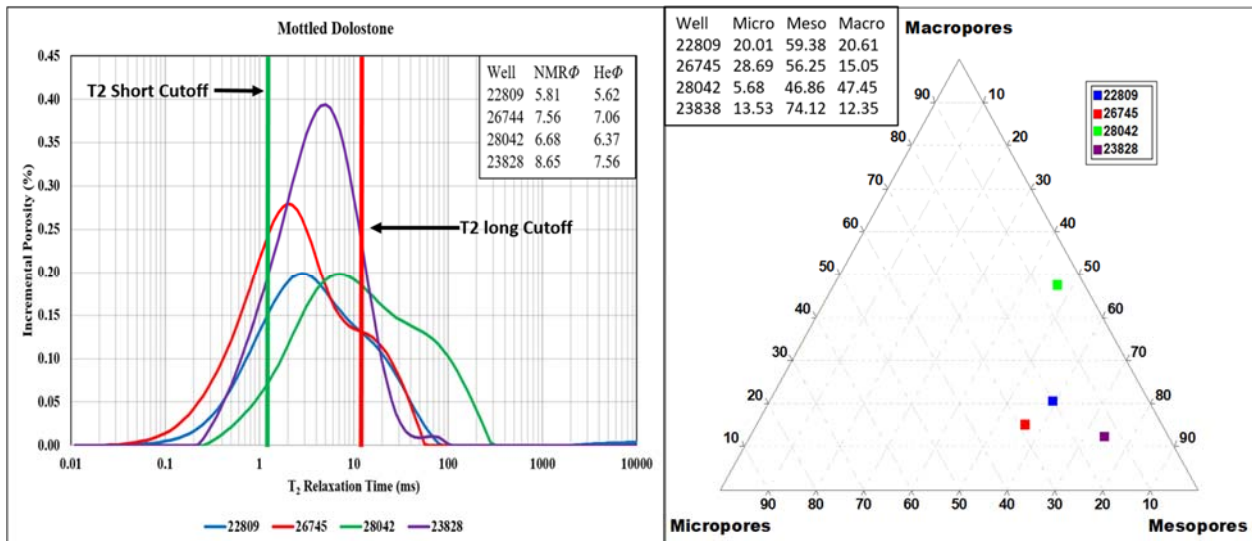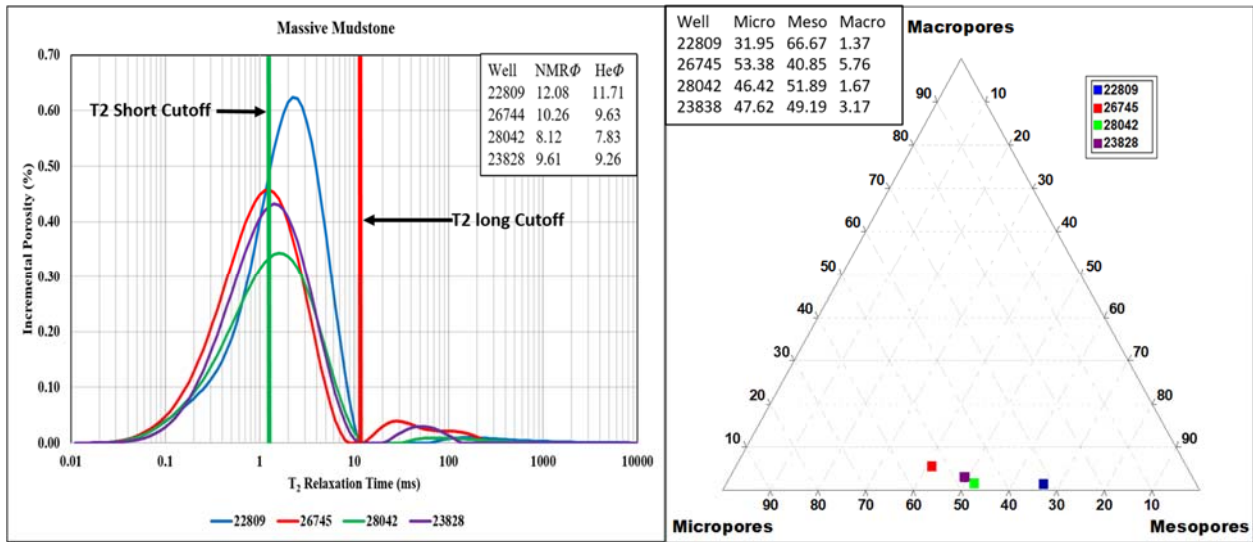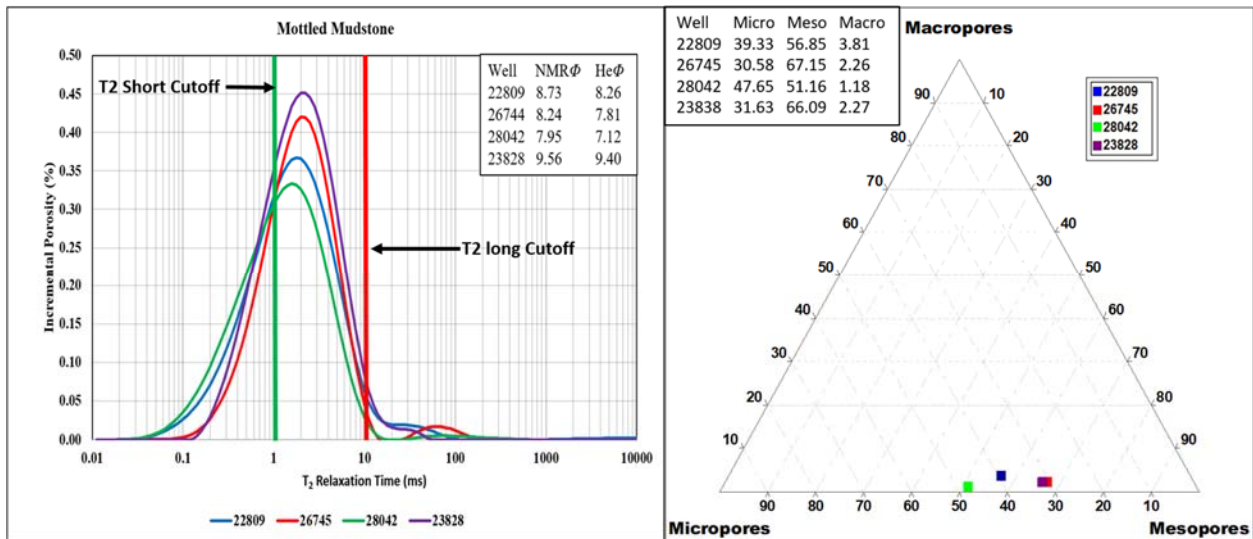

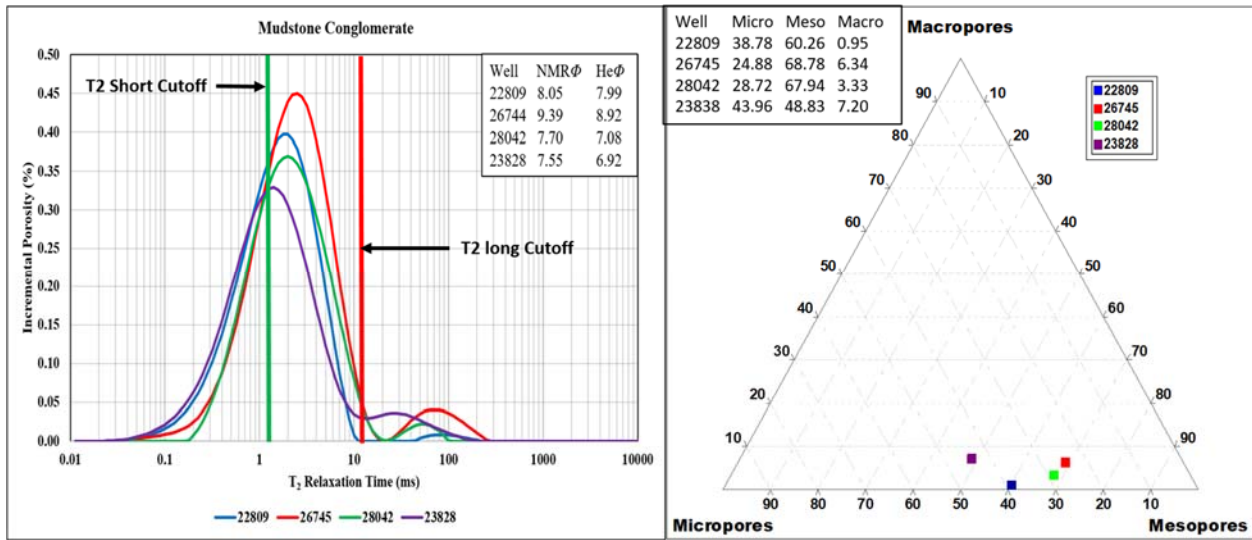Figure 49. NMR Porosity distribution and percentage of pore types in the mottled mudstone lithofacie

Figure 50. NMR Porosity distribution and percentage of pore types in the mudstone conglomerate lithofacie
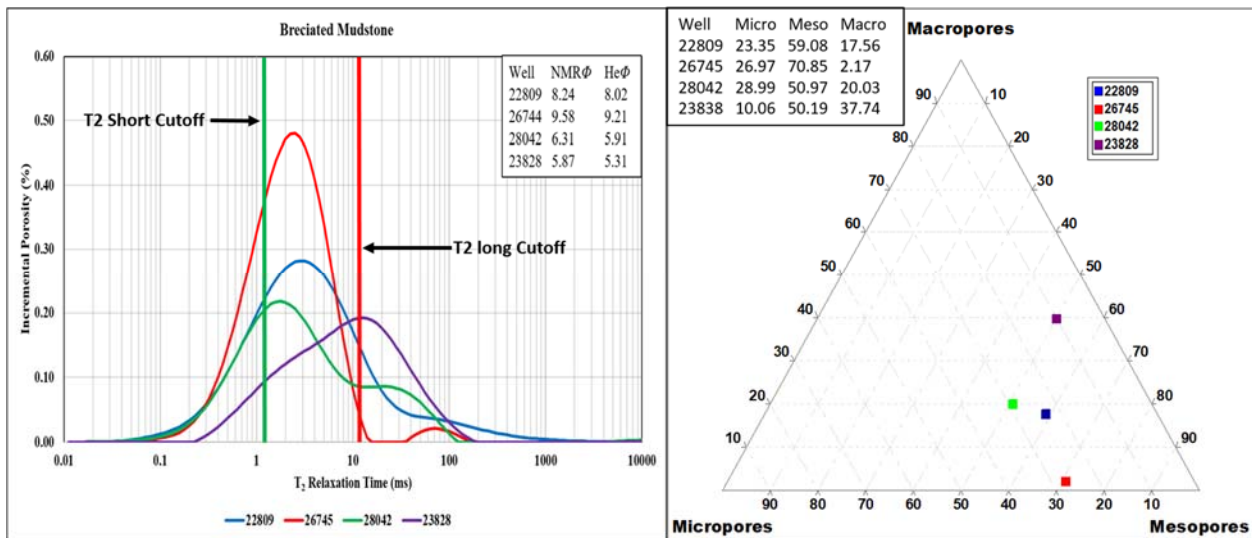

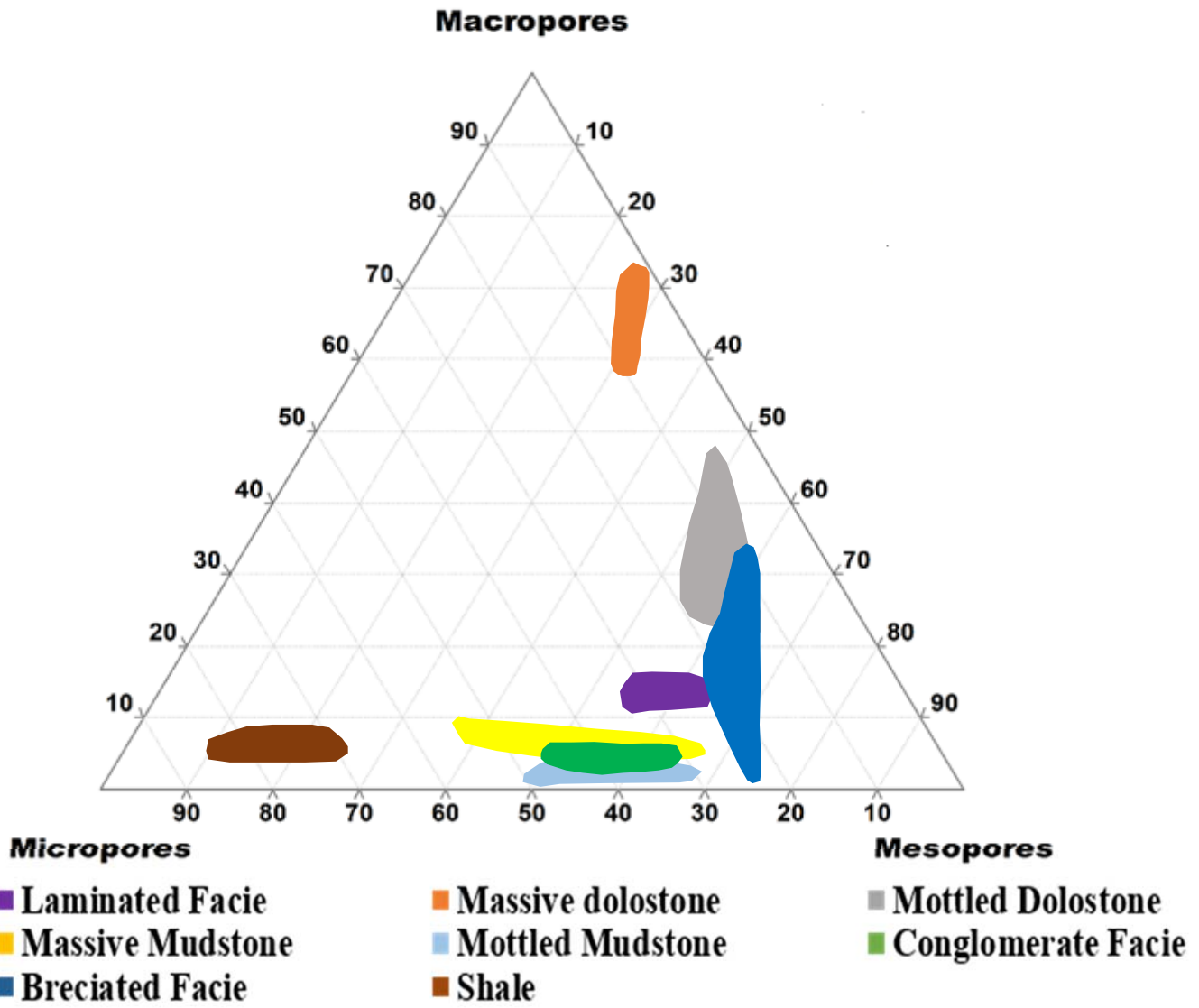Figure 51. NMR Porosity distribution and percentage of pore types in the brecciated mudstone lithofacie

Figure 52. Pore sizs distribution within lithofacies across study wells

Saturation

The fluid saturation results from standard core analysis were compiled from the North Dakota Industrial Commission (NDIC) online database. The facies were tied to the saturation results from all wells with their respective depths. The relationship between fluid saturation in the Three Forks lithofacies can be explained with variations in pore sizes distribution. The variation in saturation within the same facies across the wells is controlled by the thermal maturity and hydrocarbon generation from the overlying Lower Bakken Shale. Table 10, 11, 12 and 13 show the compiled fluid saturation and porosity from the NDIC database and this study. Figure 51 and 52 shows oil and water saturation in the lithofacies across the wells.

From Figure 53, oil saturation is generally high in the Lower Bakken shale, massive dolostone and mottled dolostone. The high saturation in the Lower Bakken Shale is attributed to shale being the source bed for generation and not all generated hydrocarbon migrates away from the source bed. In addition, the dolostone lithofacies have higher oil saturation because of their high proportions of macropores and mesopores with few micropores. These pores are large enough to support the storage and transportation of movable fluids. Well 23828 has oil in the shale and massive dolostone lithofacies alone because the source rock in the well is not matured enough to generate much hydrocarbon for expulsion unlike the other wells. The generated hydrocarbon are retained in the shale.

Also from Figure 54, the mudstone lithofacies generally have the highest water saturation. This is because of their higher proportions of micropores, few mesopores and little to no macropores. These distribution of pores favors clay bound water and capillary bound water. In total, well 23828 has the highest water saturation and lowest oil saturation which is attributed to low source maturity and generation.

Table 10. Porosity and saturation of facies in well 22809

Well #22809	Depth	Oil sat	Wat sat	Core Φ	NMR Φ				He Φ
	(ft)	%	%	%	Total	Micro	Meso	Macro	
Shale	7955	6.8	67.2	5.2	3.99	3.08	0.65	0.25	3.31
Laminated	8033	3.1	74.8	6.1	5.24	1.63	2.99	0.61	4.28
Massive dolostone	7993	34.4	21.3	7.2	4.69	0.165	1.28	1.28	3.24
Mottled dolostone	7990	15.4	18.6	3.2	5.81	1.16	3.45	1.2	5.62
Massive mudstone	7998	7.5	74.5	7.4	12.08	3.86	8.05	0.16	11.71
Mottled mudstone	8024.3	2.8	90.3	4.9	8.73	3.43	4.96	0.33	8.26
Mudstone cong.	8006	0	89.7	6.7	8.05	3.12	4.85	0.1	7.99
Brec mudstone	8030	1.2	85.3	6.2	8.24	1.92	4.67	1.45	8.02

Table 11. Porosity and saturation of facies in well 26745

Well #26745	Depth	Oil sat	Wat sat	Core Φ	NMR Φ				He Φ
	(ft)	%	%	%	Total	Micro	Meso	Macro	
Shale	8708	27.65	25.92	5	2.96	2.08	0.72	0.15	2.88
Laminated	8765.5	2.47	27.47	3.61	4.73	1.11	2.99	0.62	4.26
Massive dolostone	8728.6	8.96	10.24	3.87	4.16	0.1	1.13	2.93	3.91
Mottled dolostone	8749.5	2.14	45.08	4.25	7.56	2.17	4.25	1.14	7.06
Massive mudstone	8736.2	2.16	70.8	8.13	10.26	5.48	4.19	0.59	9.63
Mottled mudstone	8762	1.46	56.67	6.04	8.24	2.52	5.53	0.19	7.81
Mudstone cong.	8739	2.21	66.24	7.94	9.39	2.34	6.46	0.1	8.92
Brec mudstone	8778				9.58	2.58	6.79	0.2	9.21

Table 12. Porosity and saturation of facies in well 28042

Well #28042	Depth	Oil sat	Wat sat	Core Φ	NMR Φ				He Φ
	(ft)	%	%	%	Total	Micro	Meso	Macro	
Shale	7970	29.45	41.58	4.73	4.25	3.06	0.92	0.26	4.01
Laminated	8023.7	0.94	65.47	5.24	6.44	2.61	2.92	0.92	6.21
Massive dolostone	7981	18	20.76	7.84	2.47	0.67	0.92	0.98	2.13
Mottled dolostone	7988	12.74	1.82	5.33	6.68	0.38	3.13	3.17	6.37
Massive mudstone	8000.1	3.39	57.69	5.86	8.12	3.77	4.22	0.14	7.83
Mottled mudstone	8014.5	0.72	74.07	5.48	7.95	3.79	4.07	0.1	7.12
Mudstone cong.	8005	1.48	69.38	6.62	7.7	2.21	5.23	0.26	7.08
Brec mudstone	8037				6.31	1.83	3.21	1.26	5.91

Table 13. Porosity and saturation of facies in well 23828

| Well #23828	Depth	Oil sat	Wat sat	Core Φ	NMR Φ				He Φ
	(ft)	%	%	%	Total	Micro	Meso	Macro	
Shale	7941	18.9	10.8	6.12	3.34	2.77	0.42	0.15	3.01
Laminated	7986	0	71	6.14	4.71	1.38	2.74	0.58	4.33
Massive dolostone	7949	33.9	31.2	8.24	2.89	0.33	1.02	1.53	2.32
Mottled dolostone	7980.2	0	85.9	2.94	8.65	1.17	6.41	1.01	7.56
Massive mudstone	7957	0	74.5	8.48	9.61	4.53	4.68	0.3	9.26
Mottled mudstone	7978	0	79.2	5.01	9.56	3.03	6.32	0.22	9.4
Mudstone cong.	7963	0	73.6	9.03	7.55	3.32	3.69	0.54	6.92
Brec mudstone	7999.2	0	74	7.47	5.87	0.59	2.95	2.33	5.31
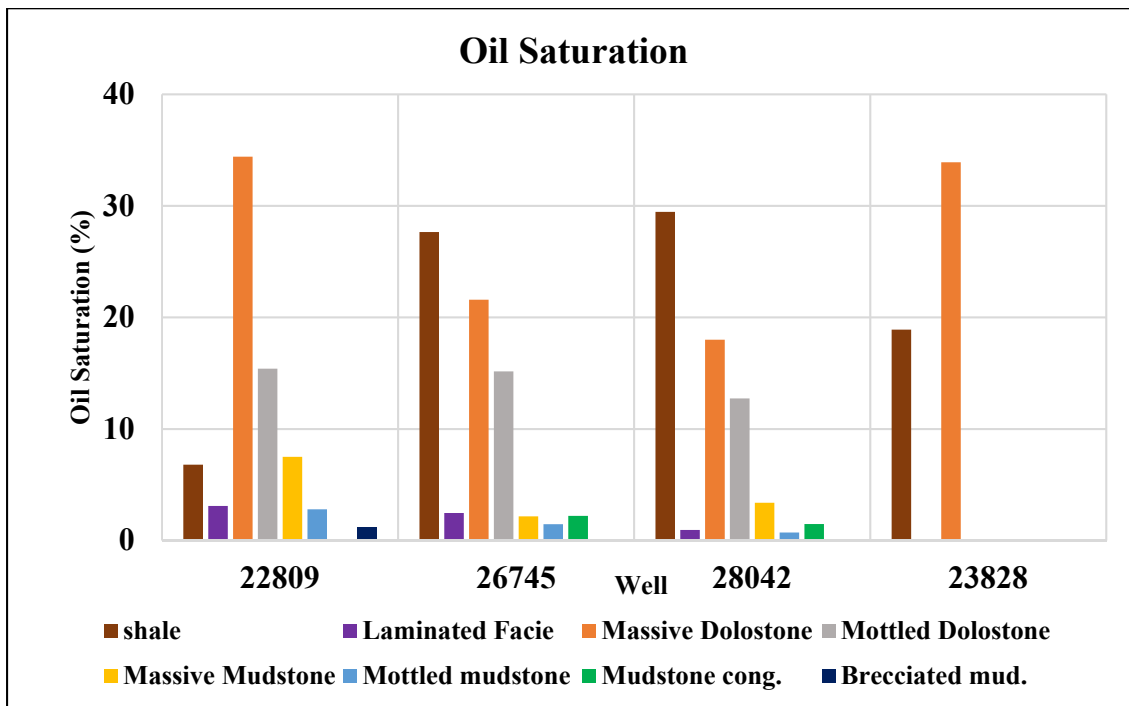
Figure 53. Oil saturation in the lithofacies.
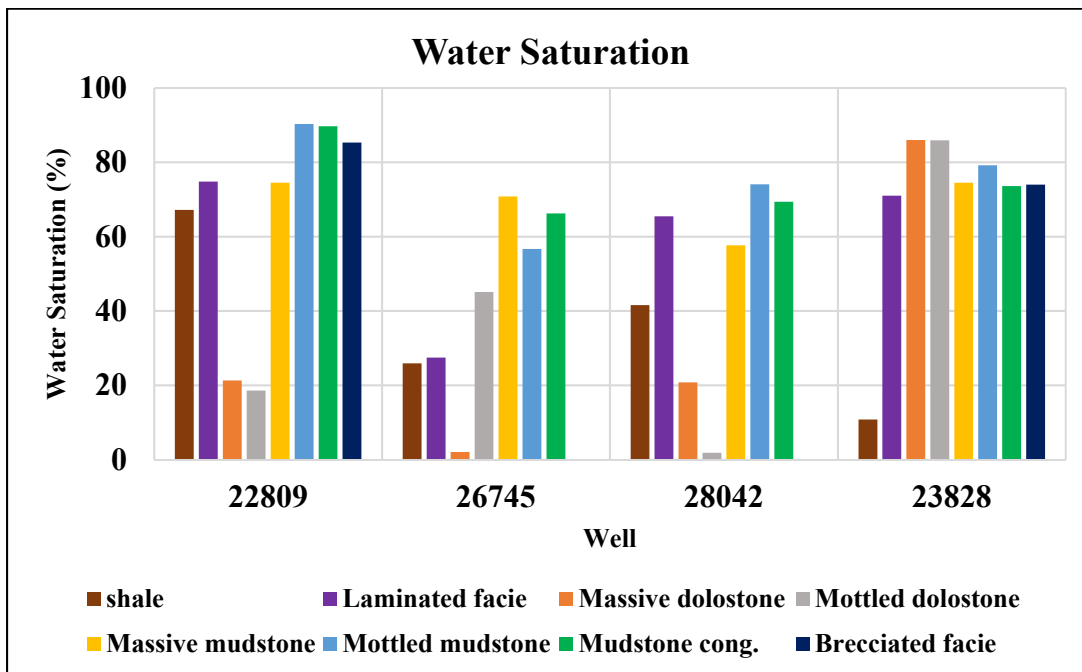
Figure 54. Water saturation in the lithofacies.

CHAPTER V

CONCLUSION

The reservoir facies identified in the Three Forks Formation that is being fed with hydrocarbon from the overlying lower Bakken Shale are 1) Laminated mudstone and dolostone; 2) Massive dolostone; 3) Mottled dolostone; 4) Massive mudstone; 5) Mottled mudstone 6) Conglomerated mudstone and 7) Brecciated mudstone.

All the wells studied have high organic carbon in the Lower Bakken Shale that is enough to generate hydrocarbon. The difference in burial depth influenced the Tmax values for maturity. They all have variable maturities with well 22809 having the highest maturity and well 23828 has the least.

The massive mudstone and mottled mudstones have the highest total porosities from both helium porosimetry and NMR method. Lower Bakken Shale, massive dolostone and laminated lithofacie have relatively low porosities. Mottled dolostone, conglomerated mudstone and brecciated mudstone have intermediate porosities. NMR porosities values are all greater that the Helium porosimetry method with a difference ranging from 1-17%, because Helium porosimetry measures the pore spaces that are penetrated by this Helium molecules. The permeability is relatively too low in these tight rocks for the Helium molecules to circulate, hence the Helium porosity are effective porosities while NMR porosities are total.

With massive dolostones having relatively very low porosities, they have the highest amounts of movable fluids due to the presence of large macropores. Massive mudstone lithofacies with highest porosities have low oil saturation, this is because most of the pores are micropores.

This proves the hypothesis to be correct i.e highest total porosity does not always result to highest saturation.

A direct relationship was established with source rock maturity and fluid saturation. The well with the most matured source rock have the highest saturation in its lithofacies and vice versa. The porosities varies for different facies and are independent of the overlying source rock maturity. Porosity distriubution influences the saturation of fluid in all the lithofacies.

REFERENCES

Abragam A. Principles of Nuclear Magnetism. Oxford: Oxford University Press; 1961.

Akkurt R, Vinegar HJ, Tutunjian PN, Guillory AJ. NMR logging of natural gas reservoirs. The Log Analyst. 1996;37:33-42.

Allen, D. F., Boyd, A., Massey, J., Fordham, E. J., Amabeoku, M. O., Kenyon, W. E., & Ward, W. B. (2001, January). The practical application of NMR logging in carbonates: 3 case studies. In SPWLA 42nd Annual Logging Symposium. Society of Petrophysicists and Well-Log Analysts.

Allen DF, Flaum C, Bed Ford J, Castelijns K, Fairhurst D, Gubelin G, et al. Trends in NMR logging. Oil Field Rev. 2000;12:2-19.

Al-Marzouqi, M. I., Budebes, S., Sultan, E., Bush, I., Griffiths, R., Gzara, K. B.,& Montaron, B. (2010). Resolving carbonate complexity. Oilfield review, 22(2), 40-55.

Ayham Ashqar. (2017) A review of the nuclear magnetic resonance physics and application in petroleum industry. Concepts in Magnetic Resonance Part A 219, e21399.

Basan P. Inroduction to NMR Petrophysics or what you need to know about NMR to survive. London, UK: LPS course; 2010.

Bottjer, R. J., Sterling, R., Grau, A., & Dea, P. (2011). Stratigraphic relationships and reservoir quality at the Three Forks–Bakken Unconformity, Williston Basin, North Dakota.

Carlson, C.G., and S.B. Anderson, 1965, Sedimentary and tectonic history of North Dakota part of Williston Basin: Amer. Assoc. Petroleum Geologists Bull., v. 49, p. 1833–1846.

Coates GR, Xiao L, Prammer MG. NMR Logging: Principles and Applications. Halliburton Energy Services Publications; 1999: 251 pp.

Clementz, D. M., Demaison, G. J., & Daly, A. R. (1979, January). Well site geochemistry by programmed pyrolysis. In Offshore Technology Conference. Offshore Technology Conference.

Christopher, J.E. , 1962 , The Three Forks Group (Uppe r Devonian-Kinderhookian) of southern Saskatchewan , in A.R. Hansen and J.H . McKeever , eds. , Three Forks and Belt Mountains area, The Devonian System of Montana and adjacent areas , 13th annual field conference and symposium, Billings , Montana , Billings Geological Society, p. 67-77.

Dow, W. G. (1974). Application of oil-correlation and source-rock data to exploration in Williston Basin. AAPG bulletin, 58(7), 1253-1262.

Dumonceaux, G. M. (1984). Stratigraphy and depositional environments of the Three Forks Formation (Upper Devonian), Williston Basin, North Dakota (Doctoral dissertation, University of North Dakota).

Espitalie, J., Madec, M., Tissot, B., Mennig, J. J., & Leplat, P. (1977, January). Source rock characterization method for petroleum exploration. In Offshore Technology Conference. Offshore Technology Conference.

Fuller, D. J. (1956). Mississippian Rocks in the Saskatchewan Portion of the Williston Basin: A Review. Williston Basin Symposium.

Garcia-Fresca, B., Pinkston, D., Loucks, R. G., & LeFever, R. (2017). The Three Forks Playa-lake depositional model; Implications for characterization and development of an unconventional carbonate play. AAPG Bulletin, (20,171,220).

Gaswirth, S. B., & Marra, K. R. (2015). US Geological Survey 2013 assessment of undiscovered resources in the Bakken and Three Forks Formations of the US Williston Basin ProvinceResource Assessment of the Bakken and Three Forks Formations. AAPG Bulletin, 99(4), 639-660.

Gerhard, L. C., S. B. Anderson, and D. W. Fischer, 1990, Petroleum geology of theWilliston Basin, in M. W. Leighton, D. R. Kolata, D. T. Oltz, and J. J. Eidel, eds., Interior cratonic basins: AAPG Memoir 51, p. 507–559

Green, D.P. and D. Veselinovic, 2010. Analysis of unconventional reservoirs using new and existing NMR Methods, GeoCanada, Calgary, Canada, June 2010.

Hayes, M.D. (1984): Conodonts of the Bakken Formation (Devonian and Mississippian), Williston Basin, North Dakota; M.Sc. thesis, University of North Dakota, Grand Forks, North Dakota, 178p.

Haynes. W. P., 1916 , The fauna of the Upper Devonian in Montana: Part 2, The stratigraphy and the Brachiopoda: Ann. Carnegie Mus., v. 10, p. 13-54 .

Holland Jr, F. D., Hayes, M. D., Thrasher, L. C., & Huber, T. P. (1987). Summary of the biostratigraphy of the Bakken Formation (Devonian and Mississippian) in the Williston basin, North Dakota. Williston Basin Symposium.

Hunt, J. M. (1996). Petroleum geochemistry and geology (Vol. 2, pp. 1-743). New York: WH Freeman.

Jin, H., Sonnenberg, S. A., & Sarg, J. F. (2012). Source Rock Evaluation for the Bakken Petroleum System in the Williston Basin, North Dakota and Montana. AAPG Search and Discovery Article 20156.

Keating K. Linking NMR relaxation measurements to hydrogeologic state variables. 2012.www.hgg.geo.au.dk/meetings_powerpoints/Kristina_Keating_NMR_Hrydrosector_meeting_Aug_2012. pdf. Accessed March 5, 2013.

Korringa J, Seevers DO, Torrey HC. Theory of spin pumping and relaxation in systems with a low concentration of electron spins resonance centers. Phys Rev. 1962;127:1143-1150.

Kume, J. (1963). The Bakken and Englewood Formations of North Dakota and northwestern South Dakota.

Leckie, D. A., Kalkreuth, W. D., & Snowdon, L. R. (1988). Source rock potential and thermal maturity of Lower Cretaceous strata: Monkman Pass area, British Columbia. AAPG Bulletin, 72(7), 820-838.

LeFever, J. A., Martiniuk, C. D., Dancsok, E. F., & Mahnic, P. A. (1991). Petroleum potential of the middle member, Bakken Formation, Williston Basin. Williston Basin Symposium.

LeFever, J., & Nordeng, S. (2015). Activity update for Bakken petroleum system, Williston Basin. Geo News.

McCabe, H.R., 1959, Mississippian stratigraphy of Manitoba , Winnipeg, Manitoba, Department of Mines and Natural Resources, Mines Branch , Publication 58-1,99 p.

Meissner, F. F. (1991). Petroleum geology of the Bakken Formation Williston Basin, North Dakota and Montana.

Meissner, F. E, 1978, Petroleum geology of the Bakken Formation, Williston basin. North Dakota and Montana, in The economic geology of the Williston basin: Montana Geological Society 24th Annual Conference; 1978 Williston Basin Symposium, p. 207-227.

Moss AK, Zacharopoulos A, de Freitas BMH. Shale volume estimates from NMR core data, SCA 2003-66; 2003.

Moss AK, Jing XD. An investigation into the effect of clay type, volume, and distribution on NMR measurements in sandstones. SCA 2001-29; 2001.

Murray, G.H., Jr. (1968): Quantitative fracture study - Sanish Pool, McKenzie County, North Dakota; American Association of Petroleum Geology Bulletin, v52,p57-65.

Nordeng, S. (2010). A brief history of oil production from the Bakken Formation in the Williston Basin. Geo News: North Dakota, Department of Mineral Resources Newsletter.

Nordeng, S. H. (2015). Compensating for the compensation effect using simulated and experimental kinetics from the Bakken and Red River Formations, Williston Basin, North Dakota (abs.). In AAPG Annual Convention and Exhibition.

Nordeng, S.H. 2010. The Bakken Petroleum System: An example of a continuous petroleum accumulation, North Dakota Industrial Commission, Department of Mineral Resources Newsletter, vol. 36, no. 1, p. 21-24.

Nordeng, S. H., & LeFever, J. A. (2009). Organic geochemical patterns in the Bakken source system. North Dakota Geological Survey.

Nordeng, S. H. (2009). The Bakken petroleum system: An example of a continuous petroleum accumulation. North Dakota Department of Mineral Resources Newsletter, 36(1), 21-24.-

Nordeng, S.H., and J.A. LeFever, 2009, Three Forks Formation log to core correlation: North Dakota Geological Survey Geologic Investigation no. 75, one plate.

NoRDQuiST, J. W. (1953). Mississippian stratigraphy of northern Montana.

Osadetz , K.G . an d L.R . Snowdon , in review , Significant Paleozoic petroleum source rocks , their distribution , richness and thermal maturity in Canadian Williston Basin (southeaster n Saskatchewa n an d southwester n Manitoba), Bulletin of the Geological Survey of Canada.

Peters, K. E. (1986). Guidelines for evaluating petroleum source rock using programmed pyrolysis. AAPG bulletin, 70(3), 318-329.

Peters, K. E., & Cassa, M. R. (1994). Applied source rock geochemistry: Chapter 5: Part II. Essential elements. The Petroleum System – From Source to Trap, AAPG Memoir 60 (1994) 93–120.

Peterson K. (2017). Pore-Size Distributions From Nuclear Magnetic Resonance And Corresponding Hydrocarbon Saturations In The Devonian Three Forks Formation, Williston Basin, North Dakota. Unpublished Masters thesis, University of North Dakota, Grand Forks, N.D., 124p.

Peterson, J. A., & MacCary, L. M. (1987). Regional stratigraphy and general petroleum geology of the US portion of the Williston Basin and adjacent areas.

Peterson, J. A. (1981). General stratigraphy and regional paleostructure of the western Montana overthrust belt.

Saskatchewan. Department of Mineral Resources, & Christopher, J. E. (1961). Transitional Devonian--Mississippian Formation of Southern Saskatchewan. Saskatchewan Department of Mineral Resources, Petroleum and Natural Gas Branch, Geology Division.

Sonnenberg, S. A. (2017) Sequence Stratigraphy of the Bakken and Three Forks Formations, Williston Basin, USA.

Sonnenberg, S. A., LeFever, J. A., & Hill, R. J. (2011). Fracturing in the Bakken petroleum system, Williston Basin.

Thrasher, L. C. 1985. Macrofossils and biostratigraphy of the Bakken Formation (Devonian and Mississippian) in western North Dakota. Unpublished Masters thesis, University of North Dakota, Grand Forks, N.D., 292p.

Tissot, B.P., and Welte, D.H. 1984. Petroleum Formation and Occurrence (2nd ed.). New York, Springer-Verlag, 699 pp.

Waples, D.W., 1985, Geochemistry in Petroleum Exploration: Boston, International Human Resources Development Corporation, 232 p

Webster, R. L. (1984). Petroleum source rocks and stratigraphy of Bakken Formation in North Dakota. AAPG Bulletin, 68(7), 953-953.

Webster, R. L., 1982, Analysis of petroleum source-rocks of Bakken Formation (lowermost Mississippian) in North Dakota (abs.): AAPG Bulletin, v. 66, p. 641.

Williams, J. A. (1974). Characterization of oil types in Williston Basin. AAPG Bulletin, 58(7), 1243-1252.